REPORT No. 627

THE EXPERIMENTAL AND CALCULATED CHARACTERISTICS OF 22 TAPERED WINGS

By Raymond F. Anderson

SUMMARY

The experimental and calculated aerodynamic characteristics of 22 tapered wings are compared, using tests made in the variable-density wind tunnel. The wings had aspect ratios from 6 to 12 and taper ratios from 1.6:1 to 5:1. The compared characteristics are the pitching moment, the aerodynamic-center position, the lift-curve slope, the maximum lift coefficient, and the curves of drag. The method of obtaining the calculated values is based on the use of wing theory and experimentally determined airfoil section data. In general, the experimental and calculated characteristics are in sufficiently good agreement that the method may be applied to many problems of airplane design.

INTRODUCTION

Considerable work has been done on the calculation of the aerodynamic characteristics of tapered wings. A method of calculating the important characteristics of tapered wings was given in reference 1 together with comparisons of experimental and calculated characteristics. It is the purpose of this report to extend reference 1 to include the calculation of the drag of all the wings contained in that report and to include the characteristics of additional wings tested in the variable-density tunnel. The additional wings comprise the 3 described in reference 2 and 10 other wings, including 7 with sections of the N. A. C. A. 230 series. Experimental lift, drag, and pitching-moment data are given and, for comparison, calculated values of pitching moment, aerodynamic-center position, lift-curve slope, maximum lift coefficient, and curves of drag.

SYMBOLS

The symbols used are as follows:

S, wing area.

b, span.

A, aspect ratio, b^2/S.

c, chord at any section along the span.

c_t, tip chord (for rounded tips, c_t is the fictitious chord obtained by extending the leading and trailing edges to the extreme tip).

c_r, chord at root of wing or plane of symmetry.

Λ, angle of sweepback, measured between the lateral axis and a line through the aerodynamic centers of the wing sections. (The symbol β was used in reference 1 but Λ has since been adopted as standard.)

ϵ, aerodynamic twist, in degrees, from root to tip, measured between the zero-lift directions of the center and the tip sections, positive for washin.

$x_{a.c.}$, longitudinal coordinate of wing aerodynamic center measured from the quarter-chord point of the root section.

a, wing lift-curve slope, per degree.

a_0, section lift-curve slope, per degree.

$\alpha_{l_{0_s}}$, angle of zero lift of the root section.

$\alpha_{s_{(L=0)}}$, wing angle of attack for zero lift, measured from root chord.

c_l, section lift coefficient; $c_l=c_{l_a}+c_{l_b}$

c_{l_b}, part of lift coefficient due to aerodynamic twist (computed for $C_L=0$).

c_{l_a}, part of lift coefficient due to angle of attack at any C_L; $c_{l_a}=C_L c_{l_{a1}}$

$c_{l_{a1}}$, part of lift coefficient due to angle of attack for $C_L=1.0$; $c_{l_{a1}}=\frac{S}{cb}L_a$

L_a, additional load distribution parameter.

$c_{m_{a.c.}}$, section pitching-moment coefficient about section aerodynamic center.

C_{m_S}, wing pitching-moment coefficient due to the pitching moments of the wing sections.

$C_{m_{a.c.}}$, wing pitching-moment coefficient about its aerodynamic center.

C_L, wing lift coefficient.

C_{D_i}, wing induced-drag coefficient.

$C_{D_e}=C_D-C_L^2/\pi A$, effective profile-drag coefficient.

E, H, J, f, factors given in reference 1.

R, Reynolds Number.

R_e, effective Reynolds Number; the Reynolds Number of variable-density-tunnel tests multiplied by the turbulence factor 2.64.

std, a subscript designating standard airfoil test results from the variable-density wind tunnel at an effective Reynolds Number of about 8,000,000.

APPARATUS AND TESTS

Standard aluminum-alloy models having an area of 150 square inches were used in the tests. In the construction of the wings, straight-line elements were used between corresponding points of the root section and the construction tip sections, except for the N. A. C. A. 23013–43010 and the elliptical N. A. C. A. 4412 wings. These wings were made by cutting several sections along the span and then fairing between the sections. The general characteristics of the models are given in table I and the principal dimensions of the plan forms, in terms of the mean chord S/b, are given

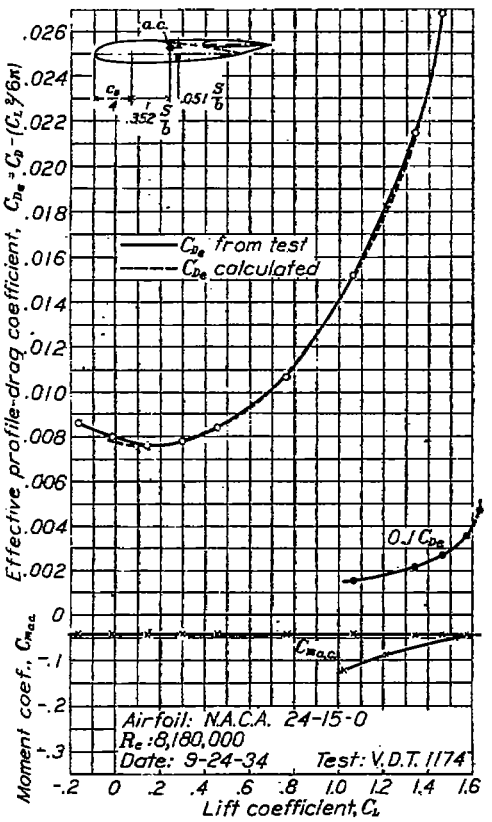

FIGURE 1.—Tapered N. A. C. A. 24-15-0 airfoil.

on the plots. The ordinates of the airfoil sections not already published in references 1, 2, and 3 are given in tables II and III.

The designating numbers of the first nine wings listed in table I are formed from numbers representing the airfoil section mean line, the sweepback, and the washout, respectively. (See reference 1.) The wings with sections of the 230 series and high aspect ratio all have a tip thickness of 9 percent of the chord and differ only in taper ratio, aspect ratio, and root thickness. Numbers representing these three quantities are therefore used to designate the wings; i. e., N. A. C. A. 3–10–18 represents a wing of 3:1 taper, aspect ratio 10, and root thickness of 18 percent.

The tests were made in the variable-density wind tunnel, which is described in reference 4. The lift, the drag, and the pitching moment of the wings were measured for positive angles of attack at a tunnel pressure of 20 atmospheres, which corresponds to a test Reynolds Number of 3,100,000 based on a 5-inch chord (effective Reynolds Number 8,200,000). The lift-curve peak was also determined for most of the wings at a lower Reynolds Number.

EXPERIMENTAL RESULTS

The results of the tests are given in figures 1 to 20 in the form of the usual dimensionless coefficients. The corrections that were applied to the tunnel data, including the method of correcting for tunnel-wall effect, are described in reference 4.

In figures 11 to 20 for the plots against angle of attack, the lift-curve peaks are given for two values of effective Reynolds Number in order to show the scale effect on $C_{L_{max}}$. The Reynolds Number is based on the mean chord S/b. In the plots against lift coefficient (figs. 1 to 20) the drag has been plotted with the minimum induced drag deducted (reference 1); thus, $C_{D_e}=C_D-\frac{C_L^2}{\pi A}$. The drag values differ from those on the plots against angle of attack in that the C_{D_e} values have been corrected to effective Reynolds Number. This correction allows for the reduction in skin friction when converting from the test to the effective Reynolds Number and amounts to a C_D increment of 0.0011 (reference 5).

The pitching-moment coefficients are given about an axis for which they are practically constant for lift coefficients up to $C_{L_{max}}$ (aerodynamic center). The aerodynamic centers were found by the method given in the appendix. The coefficients are based on the mean chord S/b in the form $C_m=\frac{M}{qS(S/b)}=\frac{Mb}{qS^2}$. The choice of a chord length for use in calculating C_m is arbitrary in any case. It is considered best, however, to use a chord length that may be conveniently found from given quantities, such as the area and the span. Coefficients so determined do not tend to be equal for wings of the same section and different taper ratios, as they would if based on the so-called "mean aerodynamic chord," but indicate directly the relative magnitude of the pitching moments of wings having equal areas and spans.

As a reference chord for the center of pressure it might appear logical to use the chord upon which the pitching-moment coefficients are based (mean chord); however, for the general case of a wing with taper and twist, if the mean chord were used, it would not be easy to decide how its location along the span and its angular attitude should be specified. The position of the root chord is known; and, as the center-of-pressure chord is simply a reference line, it was decided to base the center of pressure on the root chord.

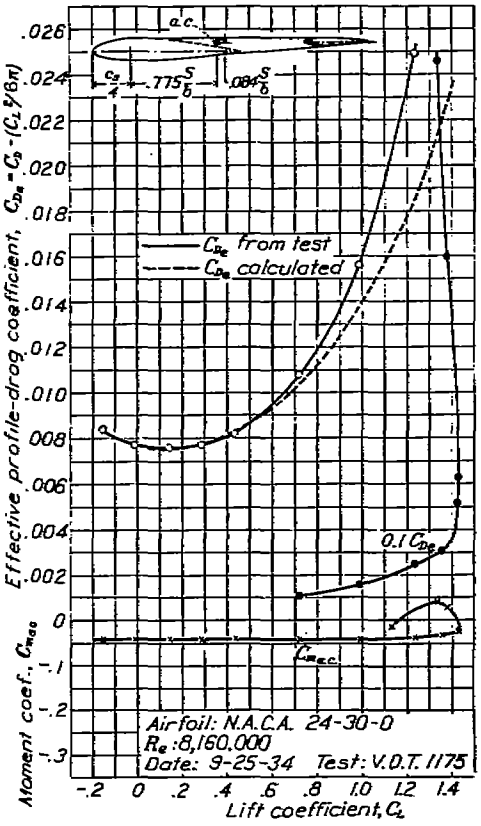

FIGURE 2.—Tapered N. A. C. A. 24-30-0 airfoil.

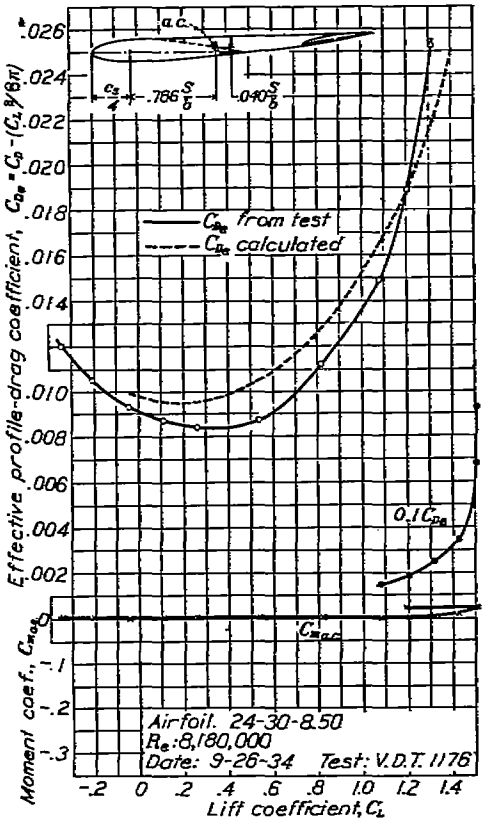

FIGURE 3.—Tapered N. A. C. A. 24-30-8.50 airfoil.

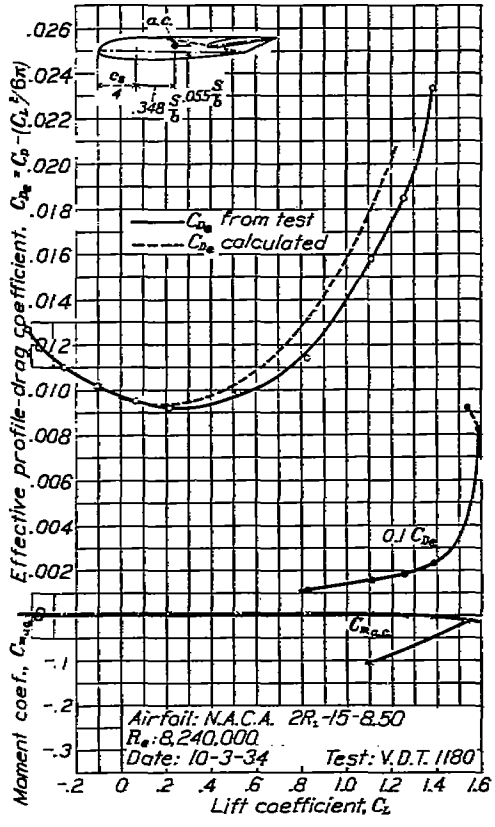

FIGURE 4.—Tapered N. A. C. A. $2R_1$-15-8.50 airfoil

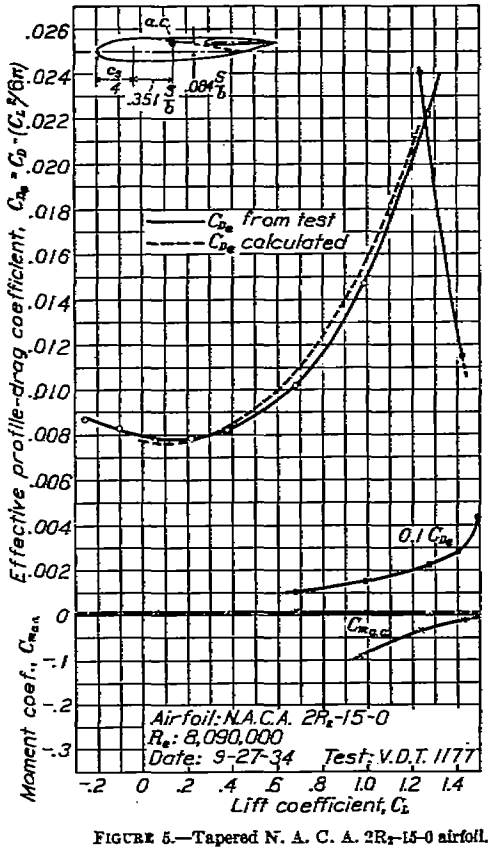

FIGURE 5.—Tapered N. A. C. A. $2R_2$-15-0 airfoil.

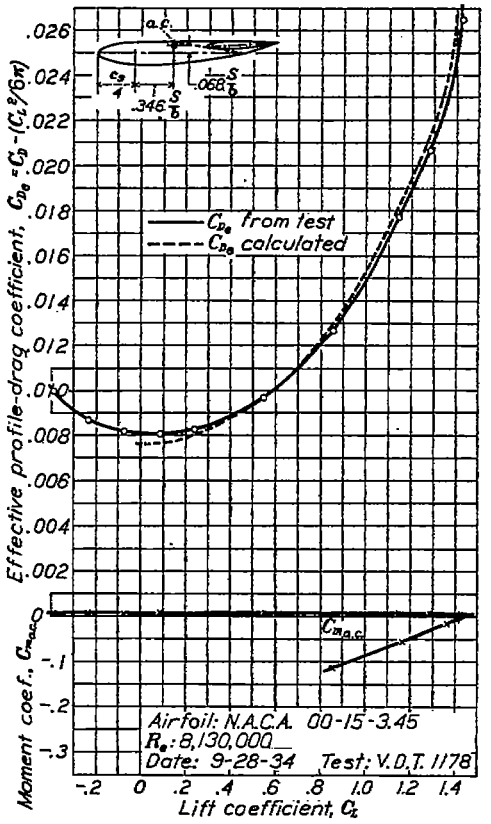

FIGURE 6.—Tapered N. A. C. A. 00-15-3.45 airfoil.

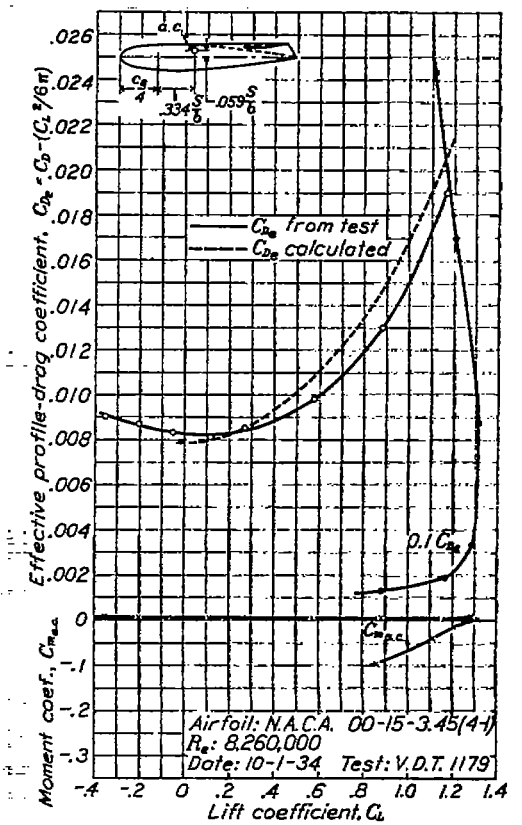

FIGURE 7.—Tapered N. A. C. A. 00-15-3.45 (4:1) airfoil.

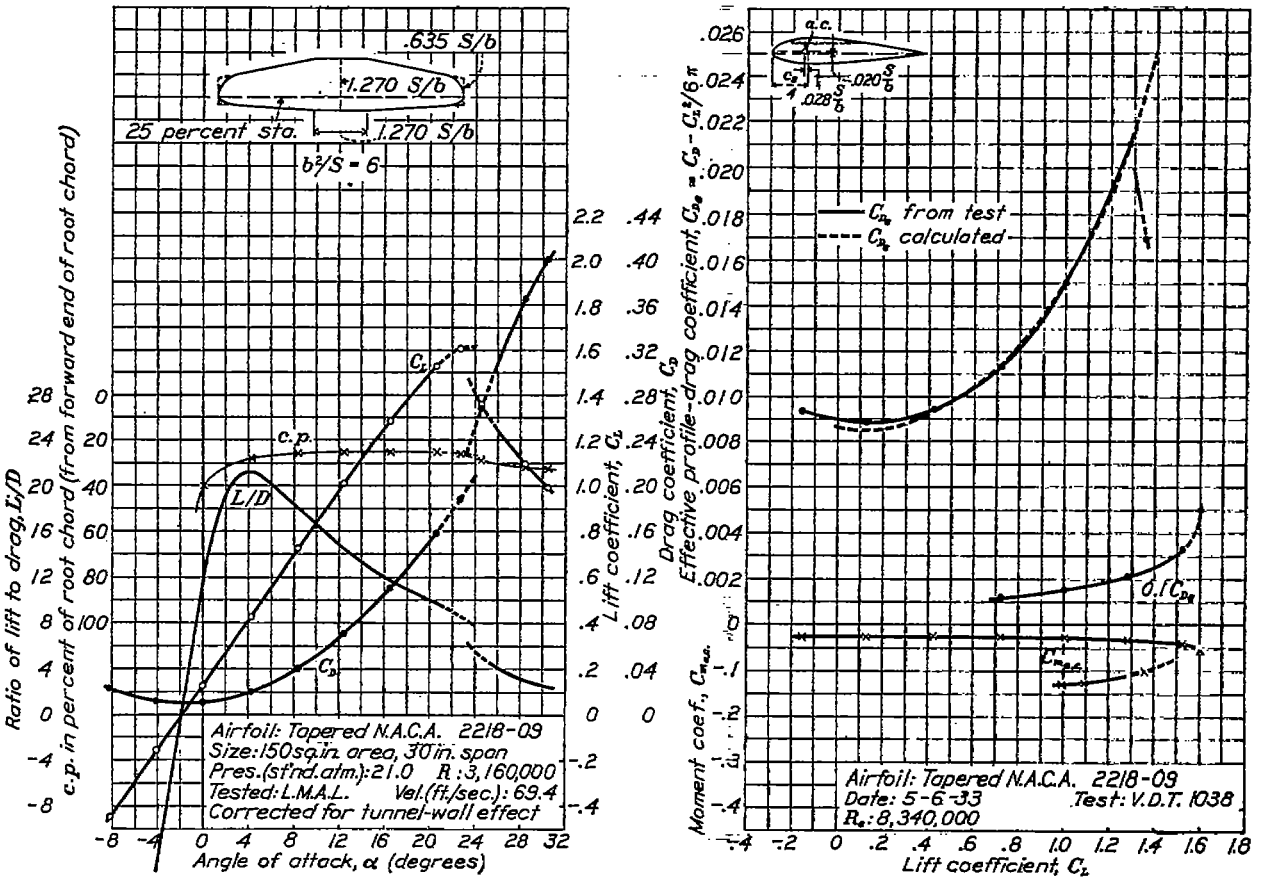

FIGURE 8.—Tapered N. A. C. A. 2218-09 airfoil.

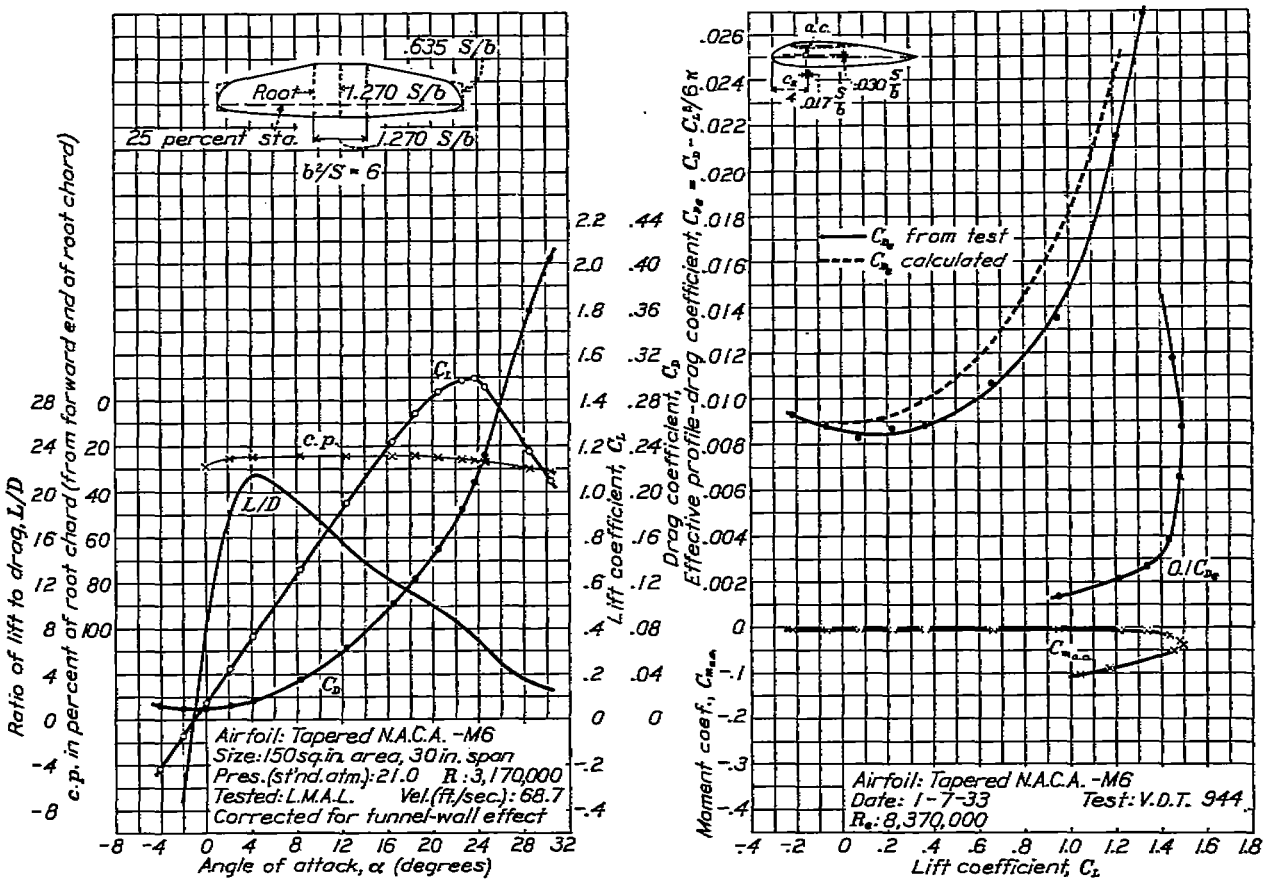

FIGURE 9.—Tapered N. A. C. A.-M6 airfoil.

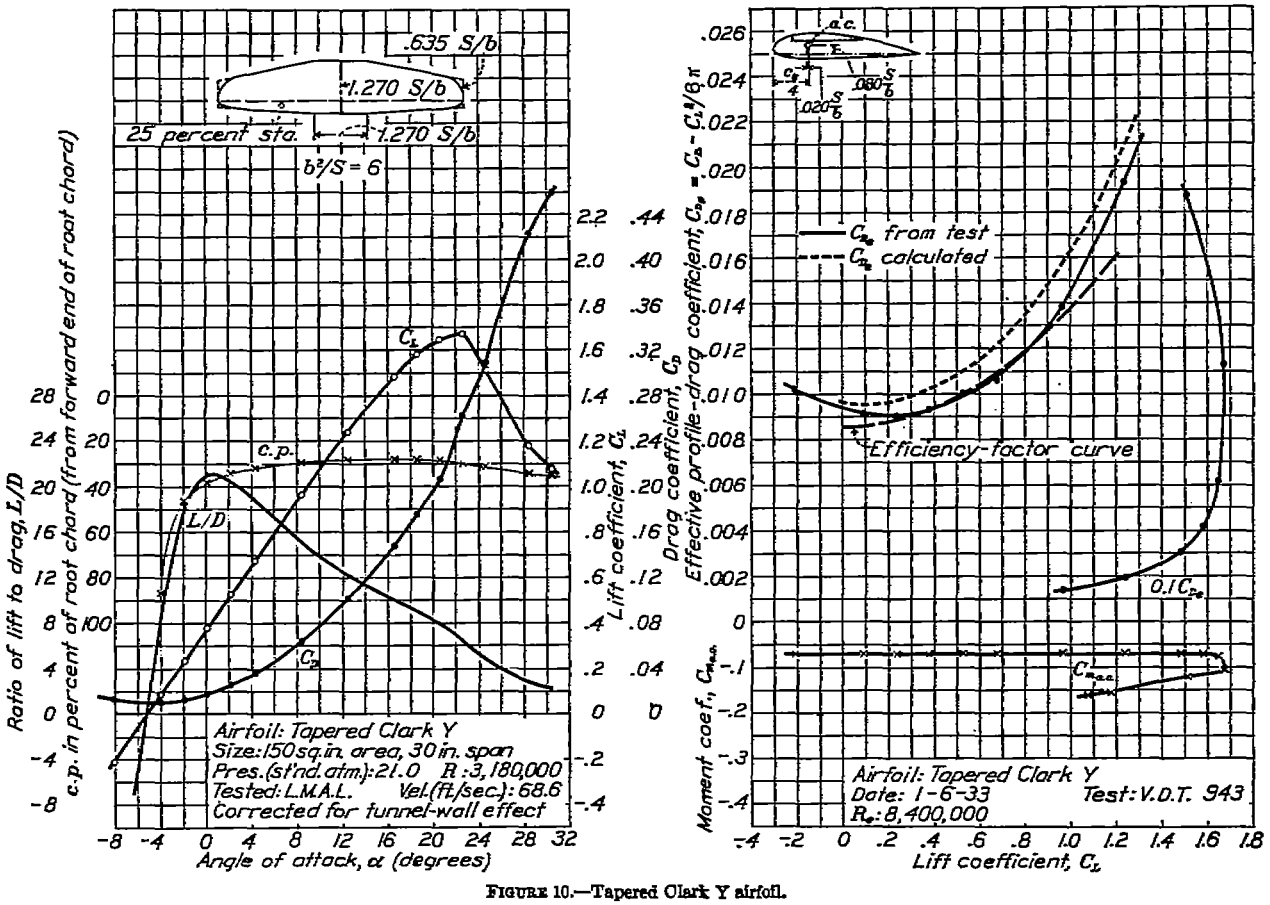

FIGURE 10.—Tapered Clark Y airfoil.

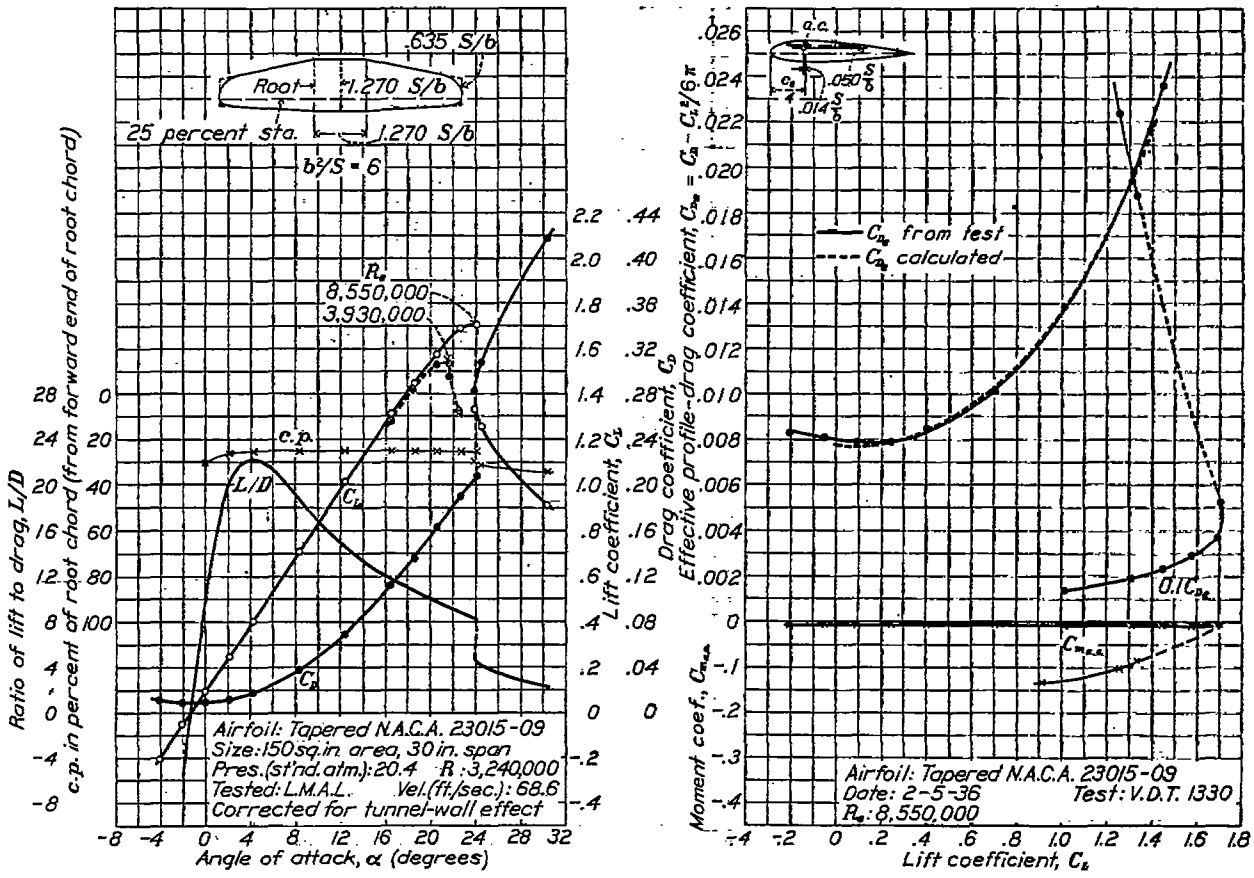

FIGURE 11.—Tapered N. A. C. A. 23015-09 airfoil.

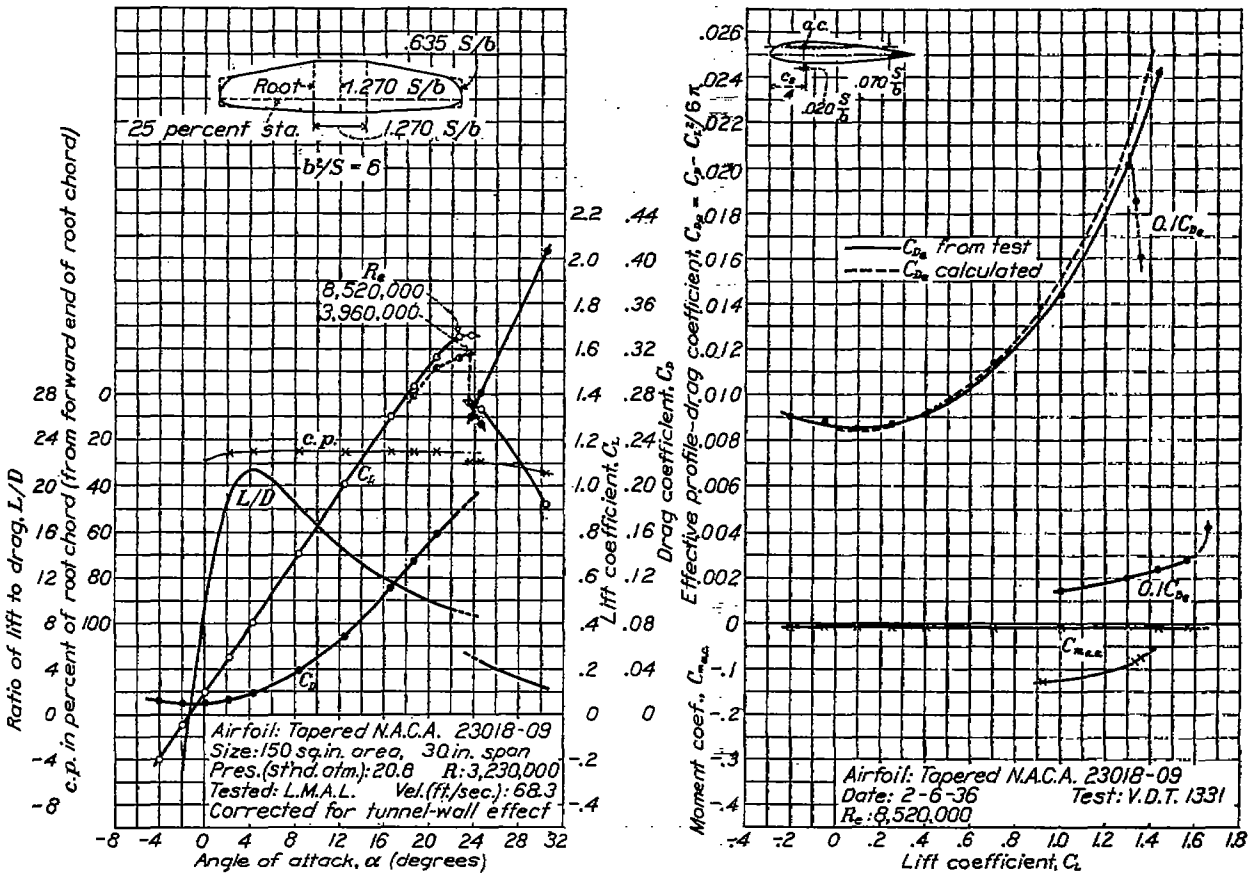

FIGURE 12.—Tapered N. A. C. A. 23018-09 airfoil.

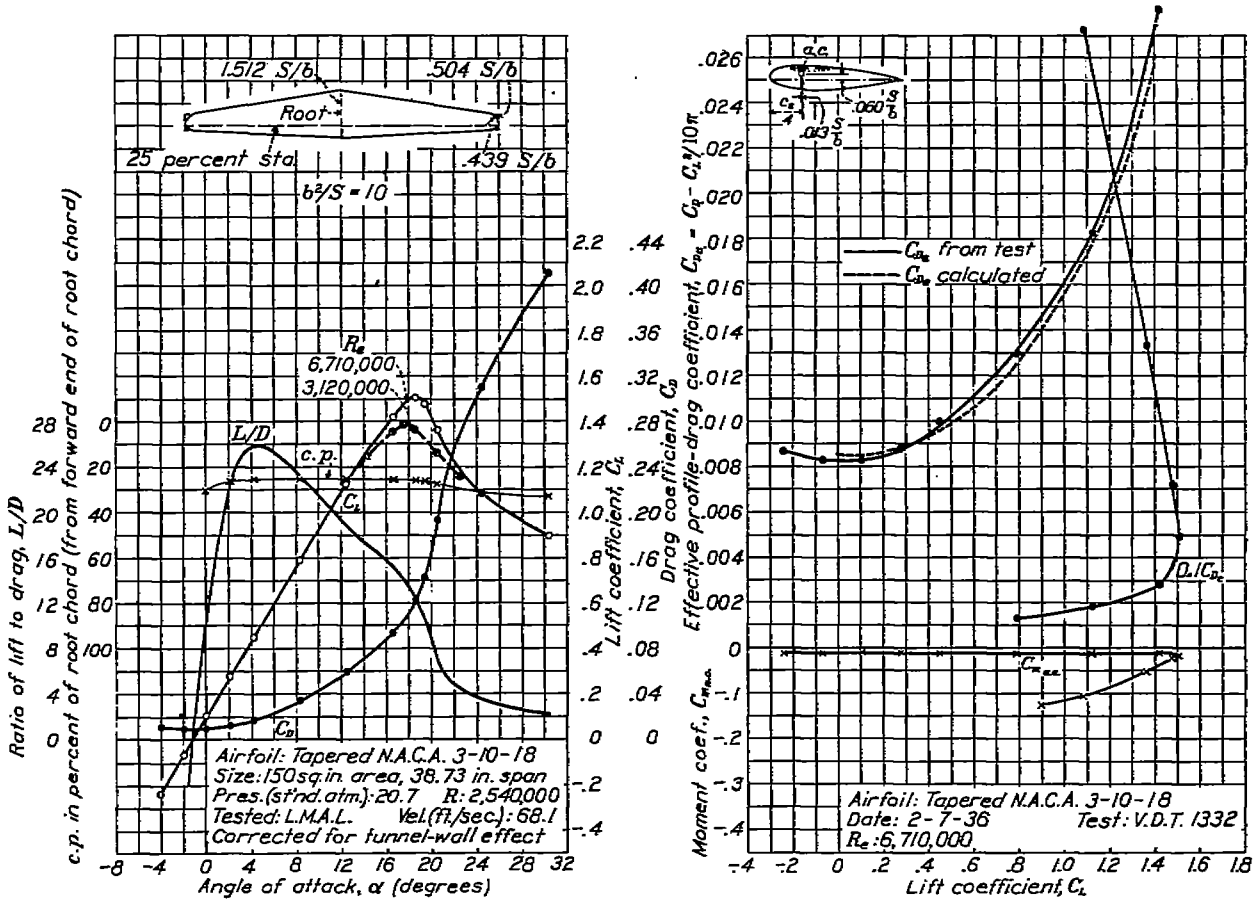

FIGURE 13.—Tapered N. A. C. A. 3-10-18 airfoil.

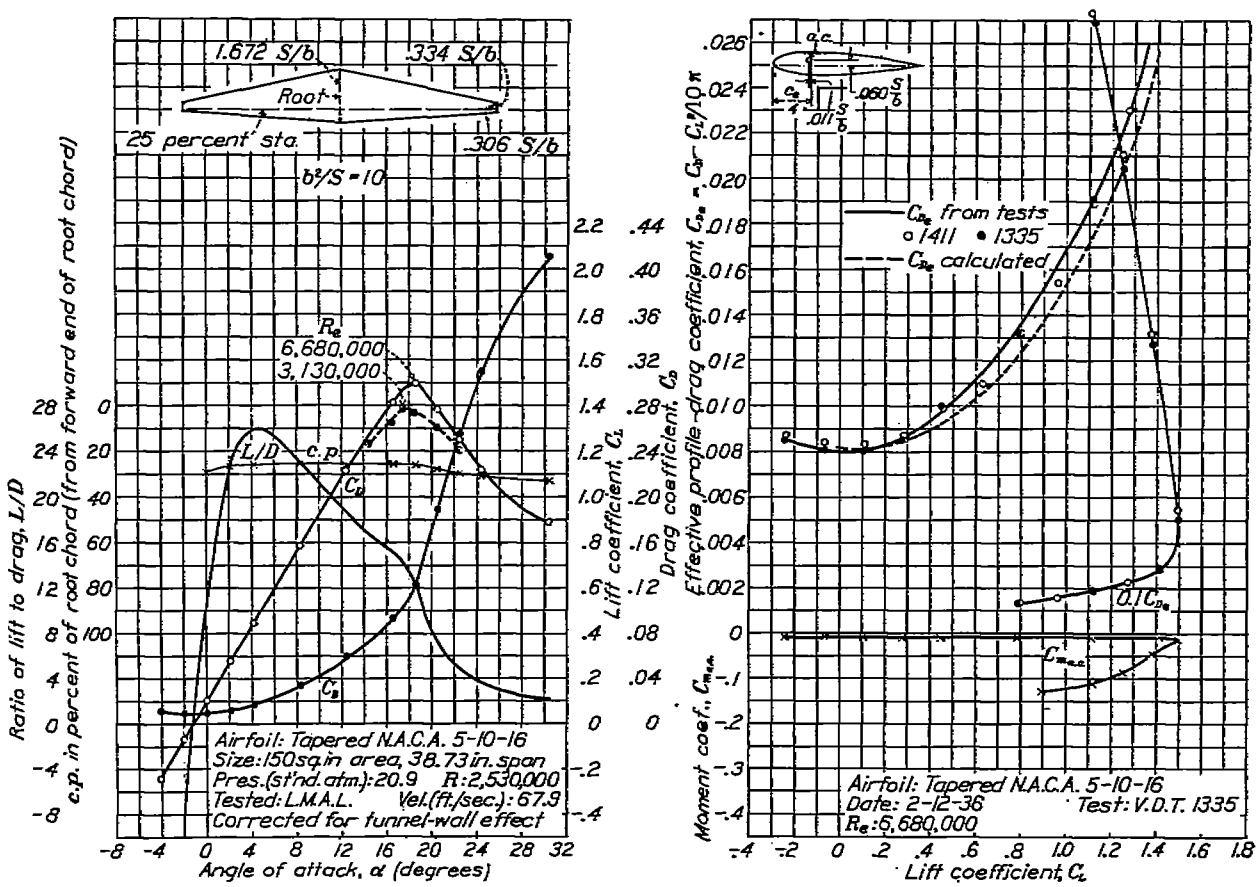

FIGURE 14.—Tapered N. A. C. A. 5-10-16 airfoil.

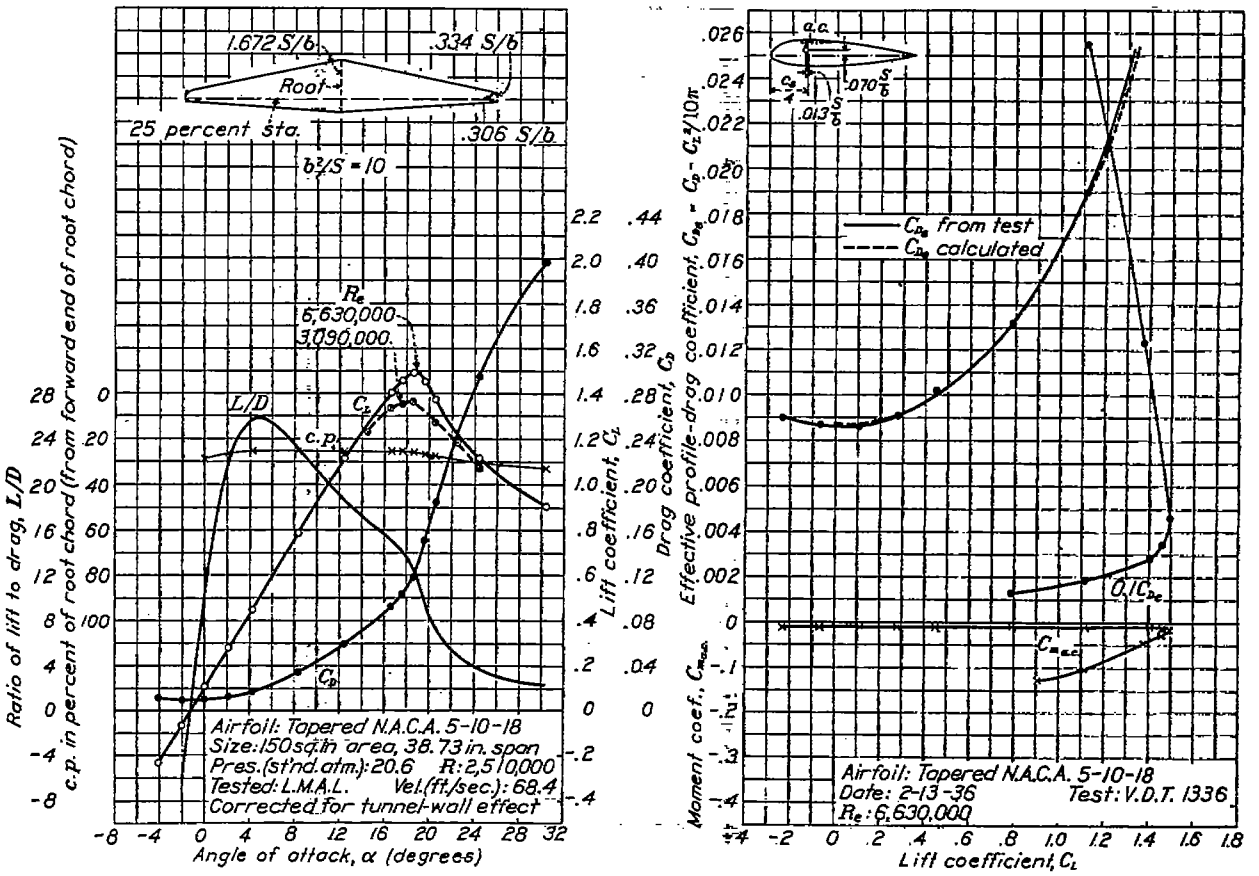

FIGURE 15.—Tapered N. A. C. A. 5-10-18 airfoil.

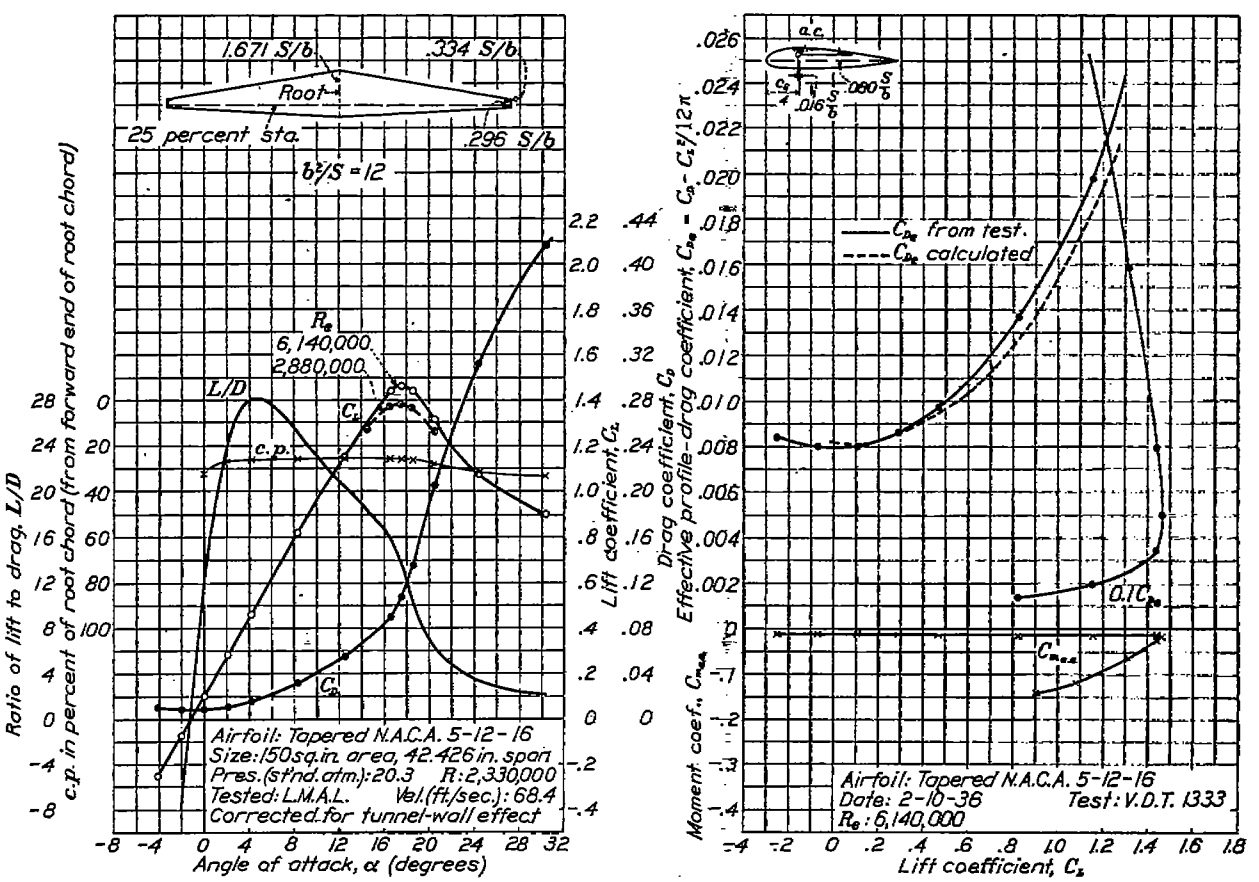

FIGURE 16.—Tapered N. A. C. A. 5-12-16 airfoil.

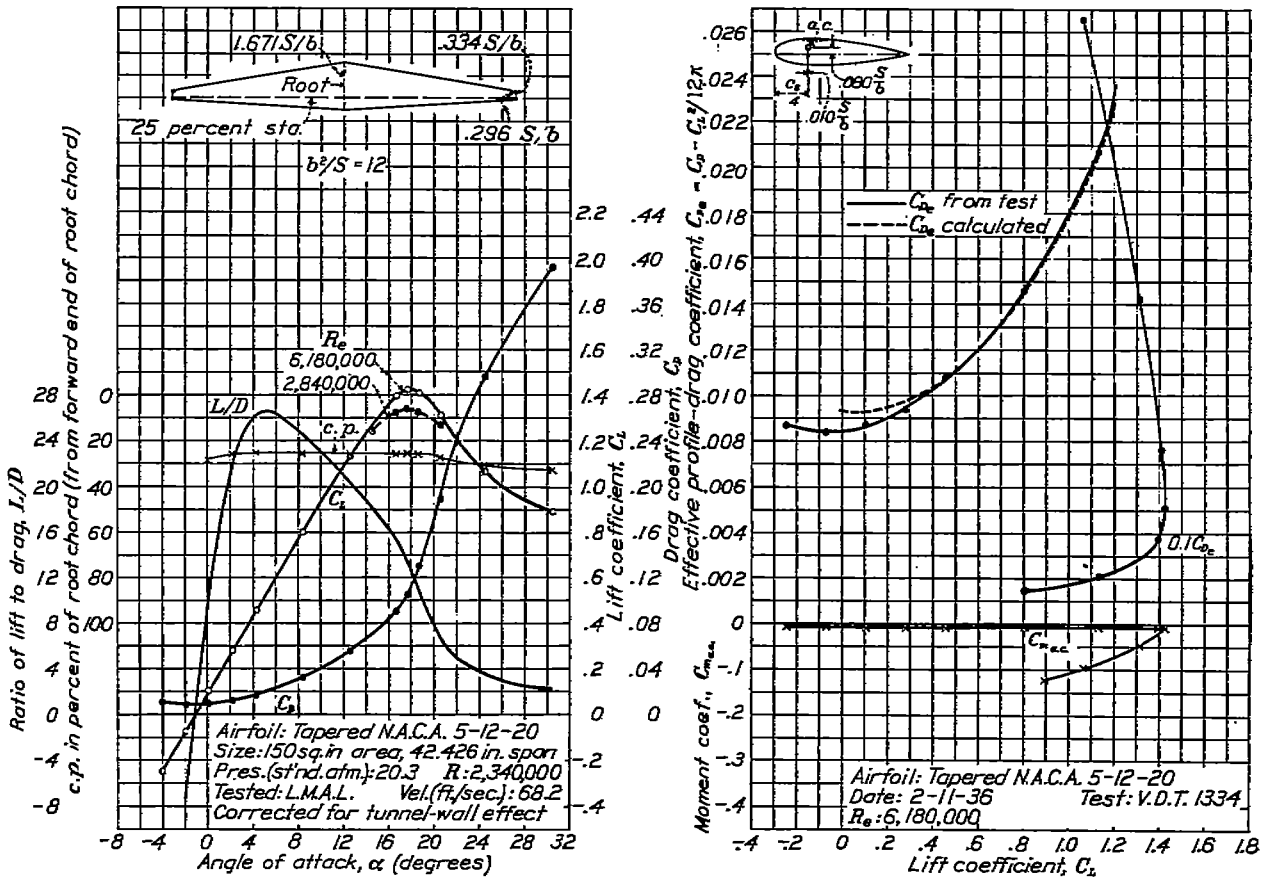

FIGURE 17.—Tapered N. A. C. A. 5-12-20 airfoil.

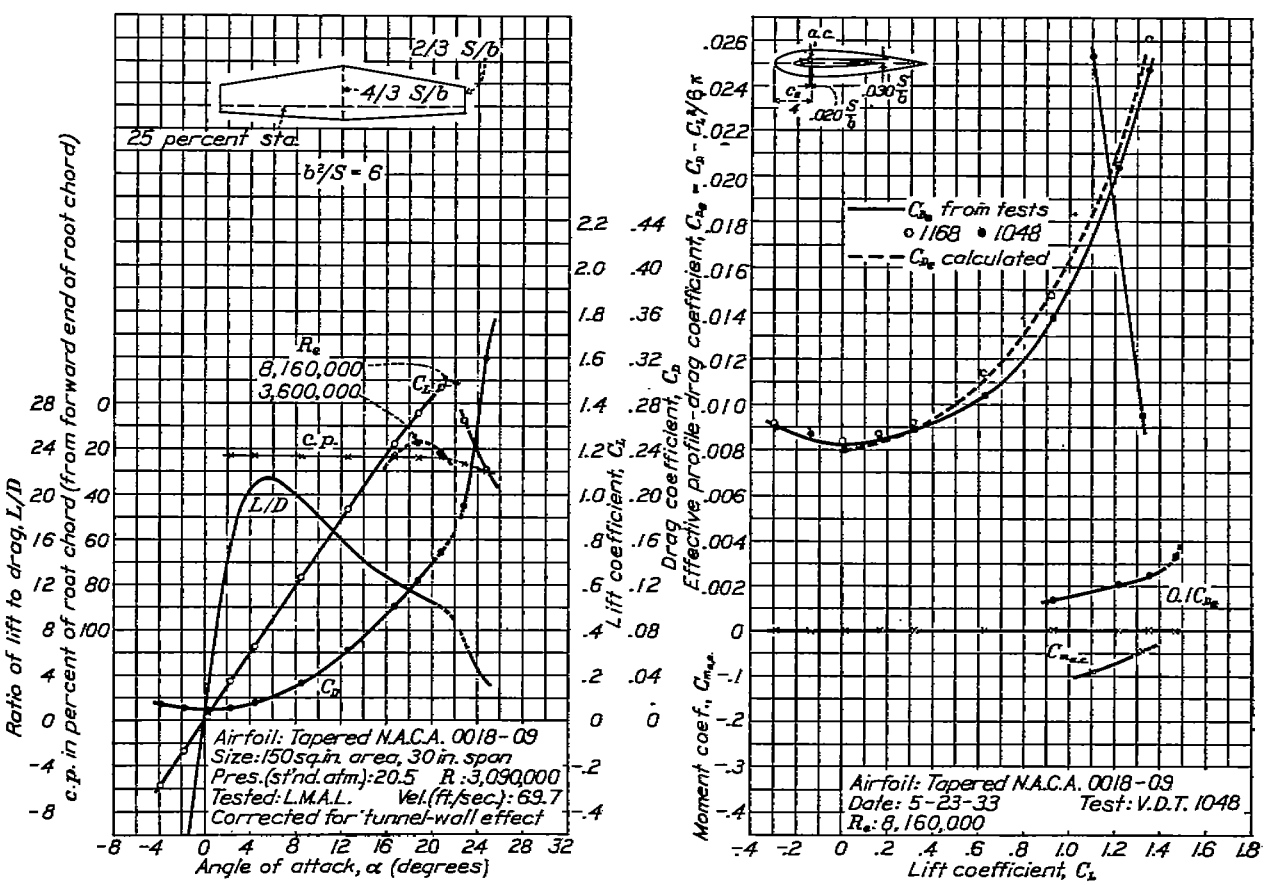

FIGURE 18.—Tapered N. A. C. A. 0018-09 airfoil.

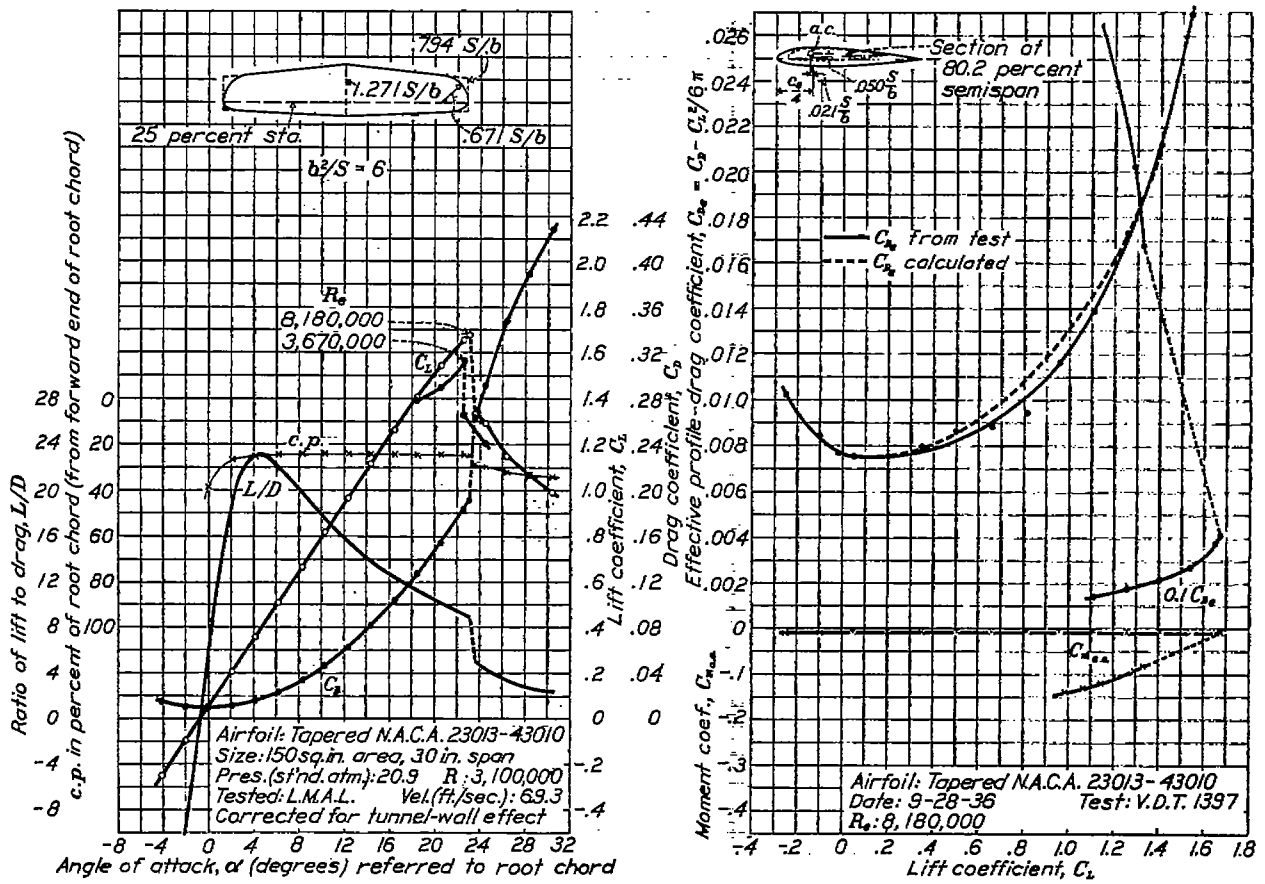

FIGURE 19.—Tapered N. A. C. A. 23013-43010 airfoil.

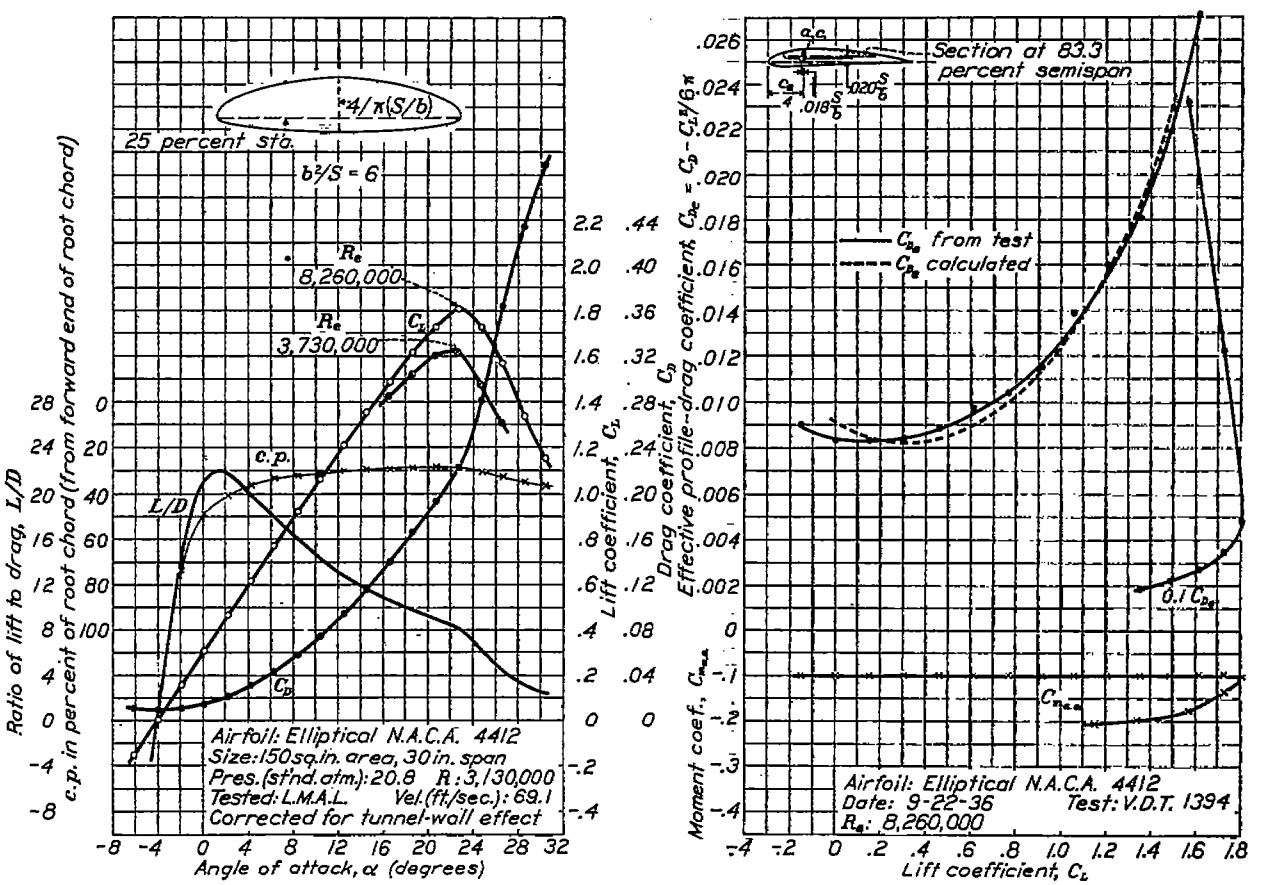

FIGURE 20.—Elliptical N. A. C. A. 4412 airfoil.

Inasmuch as the plots of lift, drag, and center of pressure against angle of attack for the first nine wings listed in table I and the plots of calculated C_{D_e} against C_L of the first two wings listed are given in reference 1, these data have been omitted from this report.

CALCULATED RESULTS

The general method of obtaining the calculated results is fully outlined in reference 1. The formulas are summarized here for convenience:

$$C_{m_{a.c.}}=C_{m_S}+C_{m_{l_b}} \tag{1}$$

$$C_{m_S}=Ec_{m_{a.c.}} \text{ } (c_{m_{a.c.}} \text{ constant across the span}) \tag{2}$$

$$C_{m_S}=\frac{2b}{S^2}\int_0^{b/2} c_{m_{a.c.}}c^2dy \text{ } (c_{m_{a.c.}} \text{ variable across span or nonlinear chord distribution}) \tag{3}$$

$$\frac{x_{a.c.}}{S/b}=HA \tan \Lambda \tag{4}$$

$$\alpha_{s_{(L=0)}}=\alpha_{l_{0_s}}+J\epsilon \tag{5}$$

$$a=f\frac{a_0}{1+\frac{57.3a_0}{\pi A}} \tag{6}$$

The calculation of $C_{m_{a.c.}}$ for the first nine wings of table I has already been described (reference 1). For the remaining wings, $C_{m_{l_b}}=0$ and, for those of straight taper, C_{m_S} was then calculated from the average of the root and tip section values of $c_{m_{a.c.}}$ and the factor E. For the wings with standard Army plan form for which E was not given in reference 1 and for the tapered N. A. C. A. 23013–43010 wing, where $c_{m_{a.c.}}$ varied appreciably across the span, C_{m_S} was calculated from equation (3). The results are given in table I.

The aerodynamic-center positions of the wings as calculated in reference 1 were based on a wing axis through the quarter-chord points of the airfoil sections, which is the section aerodynamic center according to thin-airfoil theory. A refinement consists in using as the wing axis a line through the experimental aerodynamic-center positions of the root and tip sections. The angle of sweepback is thereby slightly changed but the same value of H in equation (4) may still be used. Calculations using both angles of sweepback have been made (table I). Both aerodynamic-center positions have been referred to the quarter-chord point of the root chord for comparison.

In the computation of values of the lift-curve slope a, from equation (6), values of a_0 corrected to section data were used. For the 230 series of wings, the average value of a_0 was 0.098 per degree.

The effective profile-drag coefficient was calculated from the sum of the profile and induced-drag coefficients with the minimum induced-drag coefficient deducted:

$$C_{D_e}=C_{D_0}+C_{D_i}-\frac{C_L^2}{\pi A} \tag{7}$$

where

$$C_{D_0}=\frac{2}{S}\int_0^{b/2} c_{d_0}\, cdy$$

In order to show how C_{D_0} was calculated and to aid in making similar calculations, the method has been illustrated for the N. A. C. A. 5–10–18 wing. The calculations are listed in table IV and were obtained as follows:

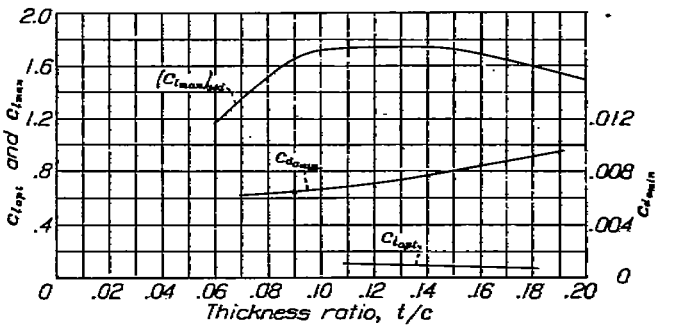

FIGURE 21.—Variation of section data with thickness. The N. A. C. A. 230 series airfoils; effective Reynolds Number, 8,200,000.

Column 1. Convenient intervals of the semispan.

Column 2. Maximum thickness of the airfoil sections at these intervals.

Column 3. Chord length.

Column 4. Effective Reynolds Number of each section along the semispan $\left(R_e=\frac{c}{S/b}6{,}630{,}000\right)$. In the case of an airplane wing the Reynolds Numbers should correspond to the particular value of C_L.

Column 5. Airfoil section maximum lift coefficient for an effective Reynolds Number of 8,200,000 as given in N. A. C. A. reports of airfoil section data. (For the method of deriving section data see reference 5, p. 17.) The value of $(c_{l_{max}})_{std}$ for the various sections along the span may be conveniently determined from a plot such as figure 21.

Column 6. Correction increment to correct the section maximum lift coefficient to the actual Reynolds Number of each section along the semispan (fig. 22). Figure 22 is figure 44 of reference 5 reproduced here for convenience.

Column 7. The maximum lift coefficient of each section along the semispan, $c_{l_{max}}=(c_{l_{max}})_{std}+\Delta c_{l_{max}}$.

Column 8. Values of minimum profile-drag coefficient for an effective Reynolds Number of 8,200,000, corrected to section data. (See reference 5.) The value of $\left(c_{d_{0_{min}}}\right)_{std}$ may be conveniently obtained by making a plot against thickness ratio, such as figure 21.

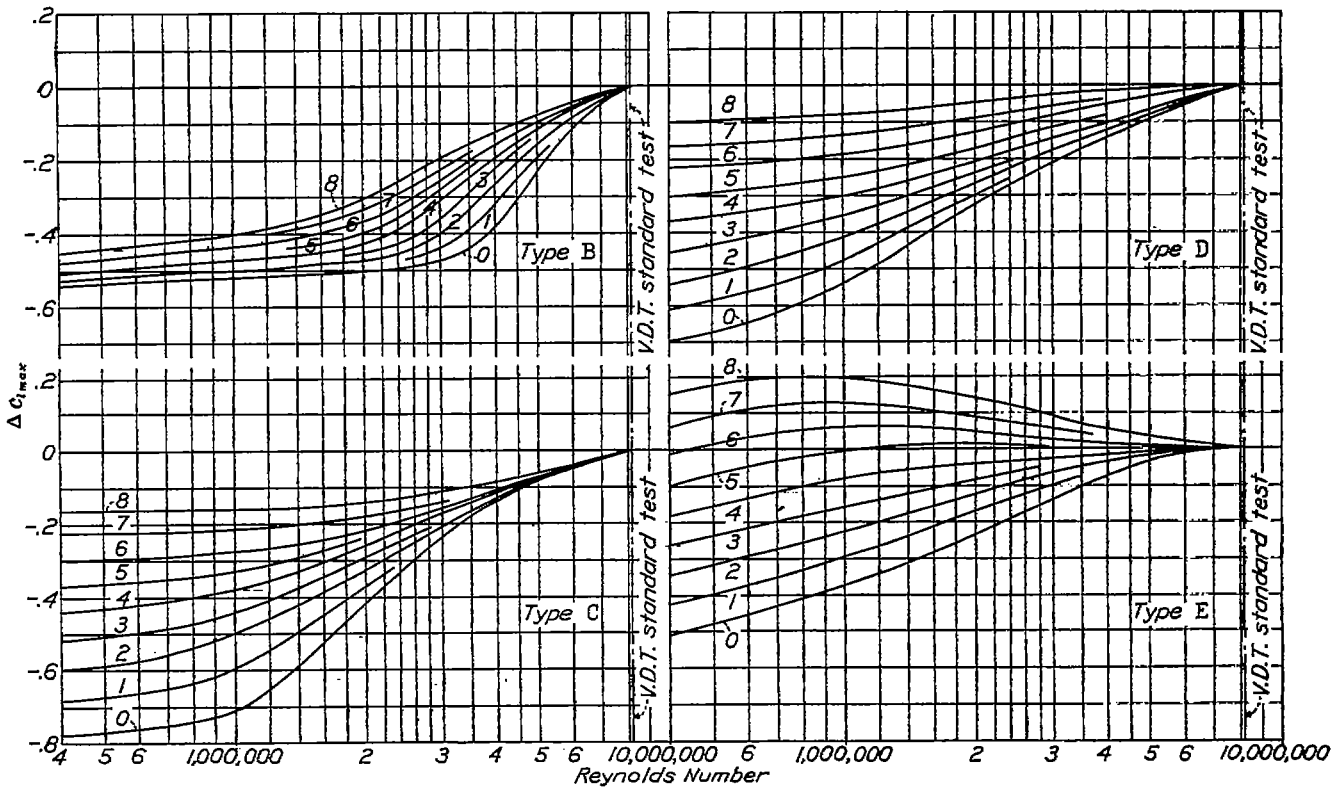

FIGURE 22.—Scale-effect corrections for $c_{l_{max}}$. In order to obtain the section maximum lift coefficient at the desired Reynolds Number, apply to the standard-test value the increment indicated by the curve that corresponds to the scale-effect designation (types B, C, D, or E) of the airfoil. (See reference 5, p. 32, and table II.)

Column 9. Values of the minimum profile-drag coefficient corrected to the Reynolds Number of each section along the semispan by use of figure 23. The basis of the correction formula is explained in reference 5. The line is plotted to provide a convenient graphi-

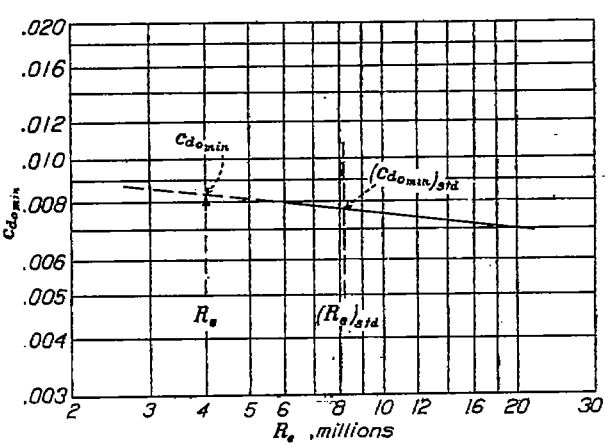

FIGURE 23.—Graph for estimating variation of $c_{d_{0_{min}}}$ with R_e.

$$c_{d_{0_{min}}} = \left(c_{d_{0_{min}}}\right)_{std}\left(\frac{(R_e)_{std}}{R_e}\right)^{0.11}$$

cal solution of the formula. The standard effective Reynolds Number of variable-density-tunnel tests is $(R_e)_{std}$. To find $c_{d_{0_{min}}}$ for any other Reynolds Number, locate the point for $\left(c_{d_{0_{min}}}\right)_{std}$ from tests in the variable-density tunnel and travel parallel to the line to the Reynolds Number in question to read the corresponding $c_{d_{0_{min}}}$. Although extrapolation by this method to Reynolds Numbers below 6,000,000 is not strictly accurate, the extrapolation has been made to 2,600,000

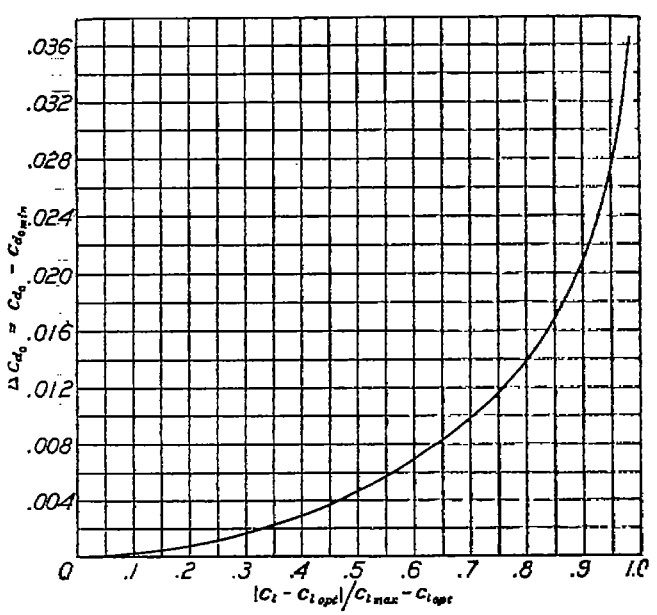

FIGURE 24.—Generalized variation of Δc_{d_0}.

for the tip sections of some of the 230 wings, as the tips contribute only a small part of the drag. The agreement of the calculated and experimental results indicates that no appreciable error was introduced.

Column 10. $c_{l_{opt}}$ is given in the tables of basic airfoil section data of N. A. C. A. reports and may be determined from a plot against thickness ratio, as in figure 21.

Column 11. $c_{l_{max}}-c_{l_{opt}}$.

Column 12. L_a is the additional load distribution parameter obtained from the tables in reference 1 for the appropriate aspect ratio and taper ratio.

Column 13. Section additional lift coefficient for a wing C_L of 1; $c_{l_{a1}}=\frac{S}{cb}L_a$.

From the foregoing basic data, the profile drag of each section along the span may now be calculated for a given wing lift coefficient. For an airplane, this lift coefficient would be the one corresponding to the speed and Reynolds Number originally assumed. The calculations are given in columns 14 to 19 for a C_L of 0.8 as follows:

Column 14. $c_l=C_L\times c_{l_{a1}}=0.8c_{l_{a1}}$. (See reference 1 for method for a twisted wing.)

Column 15. $c_l-c_{l_{opt}}$.

Column 16. $|c_l-c_{l_{opt}}|/c_{l_{max}}-c_{l_{opt}}$.

Column 17. The increment Δc_{d_0} by which c_{d_0} is increased as the lift coefficient departs from the optimum. The generalized increase for any airfoil section is obtained from figure 24. This curve was obtained from tests of airfoils of moderate camber and thickness at an effective Reynolds Number of 8,000,000 and may be applied with reasonable accuracy down to an effective Reynolds Number of 2,000,000. (See reference 5 for discussion.)

Column 18. c_{d_0} corresponding to each value of c_l along the span is $c_{d_{0_{min}}}+\Delta c_{d_0}$.

Column 19. Values of $c_{d_0}\times c$ are plotted in figure 25. The value of C_{D_0} for the wing is obtained from the area under the curve, as indicated.

The value of C_{D_i} for formula (7) was calculated from reference 1, except for the wings with standard Army plan form. For these wings the C_{D_i} and also the c_l distribution were calculated by the Lotz method. (See reference 6.)

The data given in table IV were also used for the calculation of $C_{L_{max}}$ by the method given in reference 1. The calculation is repeated here to complete the example and to give a quick method of estimating the wing maximum lift coefficient.

The maximum lift coefficients of the sections and the c_l distribution for $C_L=1.0$ are plotted as in figure 26. Stalling is considered to begin at the C_L at which c_l reaches $c_{l_{max}}$ at any point along the span. The tangent curve of c_l and the corresponding C_L are most conveniently found from the minimum value of $c_{l_{max}}/c_{l_{a1}}$ along the span, as shown. Thus, the minimum value is 1.50, which is considered to be $C_{L_{max}}$ for the wing. The measured value is 1.49. Part of the c_l curve for $C_L=1.50$ has been drawn in to show more clearly the location of the predicted stalling point. For a wing with twist, the ratio method may be used by finding the minimum value of $(c_{l_{max}}-c_{l_b})/c_{l_{a1}}$.

The calculated and experimental values of $C_{L_{max}}$ are not always in good agreement. In the case of the elliptical N. A. C. A. 4412 wing the values of $c_{l_{max}}$ of the sections decrease at the tips due to the decrease in Reynolds Number and, as c_l is constant across the span, stalling would be predicted practically at the tips at a low value of $C_{L_{max}}$. The flow near the tips is modified by the tip vortex, however, so that it is no longer two-dimensional and the method does not apply. If it were assumed that stalling begins at an arbitrary

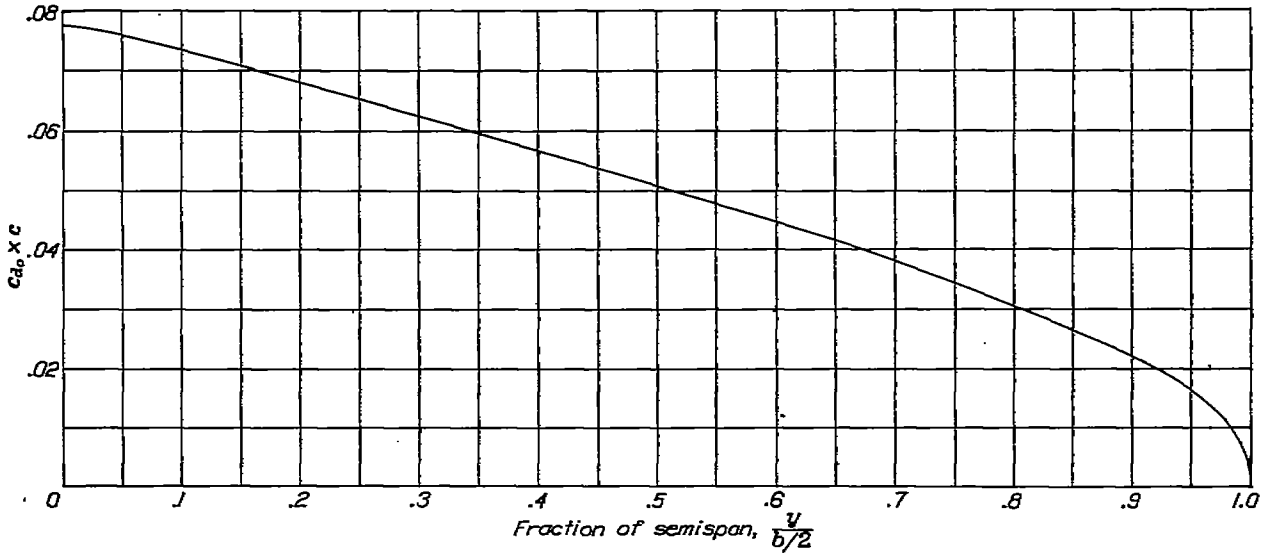

FIGURE 25.—Calculation of C_{D_0} of the N. A. C. A. 5-10-18 wing; $C_L=0.8$.

$$C_{D_0}=\frac{2}{S}\int_0^{b/2}c_{d_0}c\,dy=\frac{b}{S}\int_0^1 c_{d_0}c\,d\left(\frac{y}{b/2}\right)=\frac{33.73}{150}[(\text{area})\ (0.02)\ (0.1)]=0.0127$$

distance in from the tip equal to the chord, the predicted $C_{L_{max}}$ would be 1.74. The $C_{L_{max}}$ actually measured was 1.81, which is surprisingly high, especially as the root section $c_{l_{max}}$ is only 1.77.

For a conventional airplane in flight it is not likely that the computed $C_{L_{max}}$ would be exceeded if stalling began near the tips because of a loss of lateral control. The tapered N. A. C. A. 23013–43010 wing (fig. 19) is an example of a wing designed to avoid tip stalling. In order to cause stalling at the center, a combination of moderate taper, washout, and progression to sections having increasing $c_{l_{max}}$ (increased camber) toward the tips was used.

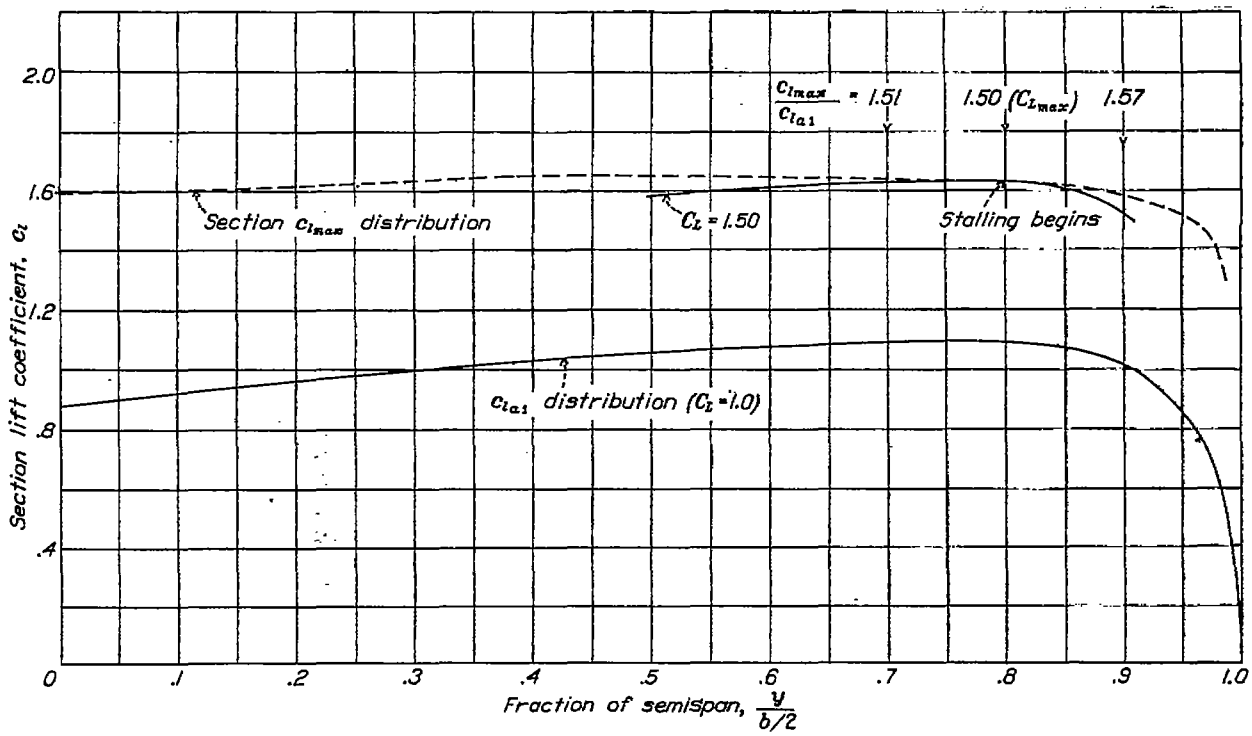

FIGURE 26.—Calculation of the C_L at which the N. A. C. A. 5-10-18 wing begins to stall.

DISCUSSION

COMPARISON OF EXPERIMENTAL AND CALCULATED VALUES

The experimental and calculated values compared in table I are, in general, in satisfactory agreement. The values of $C_{m_{a.c.}}$ are usually in agreement within the experimental error of the tests. Of the two computed values of aerodynamic-center position, better agreement is obtained by considering the lift to act at the experimental aerodynamic-center position of the sections, except for the wings with sweepback and twist. It may be concluded that for most airplane wings, which usually have little or no sweepback, it is best to calculate the wing aerodynamic-center position on the basis of the experimental section aerodynamic centers.

The angle of zero lift and the lift-curve slope need little comment except to note that for the lift-curve slope the agreement of calculated and experimental values is poorest for the N. A. C. A. 2218–09, the N. A. C. A.–M6, and the Clark Y wings and best for the wings of high aspect ratio and taper ratio and for the elliptical wing. The experimental and calculated values of $C_{L_{max}}$ are also in good agreement except for the wings with large sweepback or large twist.

Reference to the experimental and calculated C_{D_e} curves of figures 2 to 4 shows that the agreement of the C_{D_e} curves is not so good for the wings with large sweepback and large twist as for the wings with moderate or no sweepback and twist. This result would be expected, however, as the similarity of the flow conditions assumed in the calculation to the actual flow becomes less as the sweepback and twist are increased.

When the C_{D_e} curves are compared, the large scale to which they are plotted should be considered, as this factor accentuates the differences. Most of the differences do not exceed the experimental error of drag measurements, which may be as much as C_D=0.0006 for C_L=0 and may increase to 0.0015 for C_L=1.0.

Of the wings with standard Army plan form (figs. 8 to 12) only the N. A. C. A.–M6 and the Clark Y fail to show excellent agreement of the C_{D_e} curves. For these curves the greatest difference is equal to the maximum experimental error. This difference is probably due to the lack of data for sections of various thicknesses for these wings. The agreement of the C_{D_e} curves for wings with the standard Army plan form where adequate section data are available (N. A. C. A. 2218–09, 23015–09, and 23018–09 wings) is of interest because a belief has been expressed that the abrupt change in plan form at the ends of the straight center section might cause an increase in drag.

For the five wings of high aspect ratio and taper ratio (figs. 13 to 17) the C_{D_e} curves agree, in general, within the experimental error of the tests. The C_{D_e} curves for the N. A. C. A. 0018–0009, the tapered N. A. C. A. 23013–43010, and the elliptical N. A. C. A. 4412 wings (figs. 18 to 20) also show reasonably good agreement, except for a difference in the $C_{L_{opt}}$ values for the elliptical N. A. C. A. 4412 wing. It is interesting to note that for the elliptical N. A. C. A. 4412 wing there is no residual induced drag and therefore C_{D_e} is C_{D_0} for the wing.

From the C_{D_e} curves, the minimum values of C_{D_e} and the corresponding values of C_L, i. e., $C_{L_{opt}}$, are listed in table I. These values are useful for comparing the drag and lift coefficients in the high-speed region.

EFFICIENCY FACTOR

The C_{D_e} curves were analyzed with a view to finding an efficiency factor corresponding to the airplane efficiency factor used in reference 7. Incorporation of this factor in the induced-drag term permits the determination of a nearly constant drag residual over the working range of lift coefficients amounting to $C_D-\frac{C_L^2}{\pi Ae}$, which in terms of C_{D_e} is $C_{D_e}-\frac{C_L^2}{\pi A}\left(\frac{1}{e}-1\right)$.

Values of e were determined from the plots of C_{D_e} against C_L by using curves of $\frac{C_L^2}{\pi A}\left(\frac{1}{e}-1\right)$ against C_L for various values of e. The value of e was then found from the superimposed curve of $\frac{C_L^2}{\pi A}\left(\frac{1}{e}-1\right)$ that best fitted the C_{D_e} curve. The curves were made to fit as well as possible for a C_L range of 0.2 to 1.0. The values of e are given in table I. As an example of how the efficiency-factor curves fit the test or calculated curves, an efficiency-factor curve has been plotted in figure 16 for comparison with the test curve. This curve is typical for the wings and shows how the efficiency-factor curve departs from the C_{D_e} curves below $C_L=0.2$ to 0.4 and above $C_L=1.0$. Reference to table I shows that the N. A. C. A. 24–30–8.50 and $2R_1$–15–8.50 wings, which have the largest $C_{L_{opt}}$, have values of e equal to and larger than e, respectively, for the elliptical N. A. C. A. 4412 wing. This result is obtained because shifting the C_{D_e} curve to the right makes it fit a flatter e curve, and hence one with a higher value of e. If $C_{L_{opt}}$ had been zero for all the wings and they had differed only in plan form, the values of e would indicate the departure of the drag of the wings from that of the ideal elliptical wing. The wings, in fact, are sufficiently similar and the variations of the C_{D_0} values with lift are near enough alike so that there is a general reduction of e as the wings depart from the elliptical plan form toward the wings of high taper.

CONCLUSION

From the foregoing comparison of calculated and test results it may be concluded that the usual characteristics of conventional tapered wings, as determined by wind-tunnel tests, may be calculated with accuracy sufficient for use in many airplane design problems. The method of calculation should be of value for reducing wind-tunnel testing and for selecting the best wing for a given airplane design.

LANGLEY MEMORIAL AERONAUTICAL LABORATORY,
NATIONAL ADVISORY COMMITTEE FOR AERONAUTICS,
LANGLEY FIELD, VA., *November 17, 1937.*

APPENDIX

CALCULATION OF THE AERODYNAMIC-CENTER POSITION FROM EXPERIMENTAL DATA

The aerodynamic-center position of the wings and the value of $C_{m_{a.c.}}$ were determined from the test data by the following method. The forces acting at the axis about which the pitching moment is measured may be considered to be the normal and the chord forces and the pitching moment. The forces are represented as coefficients in figure 27.

For most airfoils there is some axis about which the pitching-moment coefficient may be considered constant for lift coefficients practically to $C_{L_{max}}$ (aerodynamic

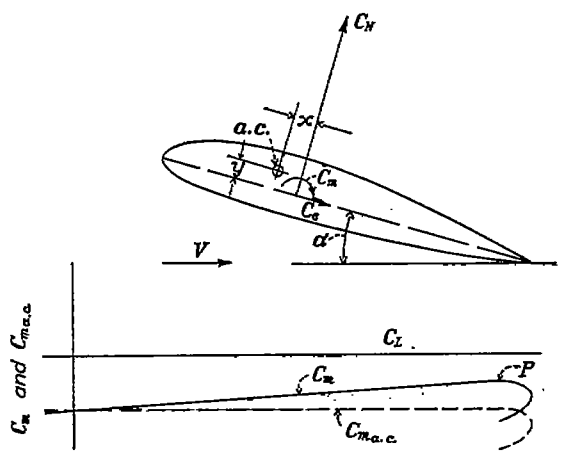

FIGURE 27.—Aerodynamic center and pitching moment.

center). The aerodynamic center is located by x and y, which are distances in terms of the mean chord S/b, i. e., $x=\frac{x_{a.c.}}{S/b}$. Then, if C_m is the pitching-moment coefficient about the support point, the pitching-moment coefficient about the aerodynamic center may be written:

$$C_{m_{a.c.}}=C_m-xC_N-yC_C \tag{1}$$

so that

$$C_m=C_{m_{a.c.}}+xC_N+yC_C \tag{2}$$

also

$$C_N=C_L\cos\alpha+C_D\sin\alpha \tag{3}$$

$$C_C=C_D\cos\alpha-C_L\sin\alpha \tag{4}$$

In order to find the three unknowns, $C_{m_{a.c.}}$, x, and y, the basic equation (2) may be used to write three equations corresponding to three conditions of the pitching-moment curve of the airfoil.

For the first condition, values of C_m, C_N, and C_C are taken for a point P on the pitching-moment curve before it curves greatly (fig. 27):

$$C_{m_P}=C_{m_{a.c.}}+xC_{N_P}+yC_{C_P} \tag{5}$$

The second condition is taken at $C_L=0$:

$$C_{m_0}=C_{m_{a.c.}}+xC_{D_{L_0}}\sin\alpha_{s_{(L=0)}}+yC_{D_{L_0}}\cos\alpha_{s_{(L=0)}} \tag{6}$$

The third condition is taken as the slope of the pitching-moment curve at $C_L=0$:

$$\frac{dC_m}{dC_L}=n_0=x\left[\left(\frac{dC_D}{dC_L}\right)_0\sin\alpha_{s_{(L=0)}}+\left(1+C_{D_{L_0}}\frac{d\alpha'}{dC_L}\right)\cos\alpha_{s_{(L=0)}}\right]$$
$$-y\left[\left(1+C_{D_{L_0}}\frac{d\alpha'}{dC_L}\right)\sin\alpha_{s_{(L=0)}}-\left(\frac{dC_D}{dC_L}\right)_0\cos\alpha_{s_{(L=0)}}\right] \tag{7}$$

where

α', is angle of attack in radians.

n, slope of pitching-moment curve, $\frac{dC_m}{dC_L}$.

P, a subscript indicating values for a point near $C_{L_{max}}$.

0 and L_0, subscripts indicating values for $C_L=0$.

The other symbols have their usual significance.

For normal airfoils, negligible error is introduced by making the approximations

$$\sin\alpha_{s_{(L=0)}}=\alpha_{s_{(L=0)}}',\ \cos\alpha_{s_{(L=0)}}=1,\ 1+C_{D_{L_0}}\frac{d\alpha'}{dC_L}=1,$$
$$\left(\frac{dC_D}{dC_L}\right)_0\sin\alpha_{s_{(L=0)}}=0,\ \left(\frac{dC_D}{dC_L}\right)_0\cos\alpha_{s_{(L=0)}}=0$$

in equations (5), (6), and (7), and the approximations

$$C_{D_{L_0}}\alpha_{s_{(L=0)}}'=0,\ C_{D_{L_0}}(\alpha_{s_{(L=0)}}')^2=0$$

when they are solved simultaneously. The solution gives x and y in the form.

$$x=\frac{(C_{m_0}-C_{m_P})\alpha_{s_{(L=0)}}'+n_0(C_{D_{L_0}}-C_{C_P})}{C_{D_{L_0}}-C_{C_P}-C_{N_P}\alpha_{s_{(L=0)}}'}$$

$$y=\frac{C_{m_0}-C_{m_P}+xC_{N_P}}{C_{D_{L_0}}-C_{C_P}}$$

When x and y have been found by substituting the appropriate test data, the $C_{m_{a.c.}}$ curve may be computed from

$$C_{m_{a.c.}}=C_m-xC_N-yC_C$$

The value of $C_{m_{a.c.}}$ is practically equal to C_{m_0} so that the $C_{m_{a.c.}}$ curve is as shown in figure 27.

REFERENCES

1. Anderson, Raymond F.: Determination of the Characteristics of Tapered Wings. T. R. No. 572, N. A. C. A., 1936.
2. Anderson, Raymond F.: Tests of Three Tapered Airfoils Based on the N. A. C. A. 2200, the N. A. C. A.-M6, and the Clark Y Sections. T. N. No. 487, N. A. C. A., 1934.
3. Jacobs, Eastman N., Ward, Kenneth E., and Pinkerton, Robert M.: The Characteristics of 78 Related Airfoil Sections from Tests in the Variable-Density Wind Tunnel. T. R. No. 460, N. A. C. A., 1933.
4. Jacobs, Eastman N., and Abbott, Ira H.: The N. A. C. A. Variable-Density Wind Tunnel. T. R. No. 416, N. A. C. A., 1932.
5. Jacobs, Eastman N., and Sherman, Albert: Airfoil Section Characteristics as Affected by Variations of the Reynolds Number. T. R. No. 586, N. A. C. A., 1937.
6. Pearson, H. A.: Span Load Distribution for Tapered Wings with Partial-Span Flaps. T. R. No. 585, N. A. C. A., 1937.
7. Oswald, W. Bailey: General Formulas and Charts for the Calculation of Airplane Performance. T. R. No. 408, N. A. C. A., 1932.

TABLE I

COMPARISON OF EXPERIMENTAL AND CALCULATED CHARACTERISTICS

Wing [1]	Plan form	Taper ratio	$\frac{c_t}{c_r}$	Aspect ratio	Root section [1]	Tip section [1]	Sweepback (degrees)	Aerodynamic twist (degrees)	$C_{m_{a.c.}}$		$\frac{F_{a.c.}}{S/b}$			$\alpha_{c_l}(L=0)$		a		$C_{L_{max}}$		$C_{D_{min}}$ at R_c		$C_{L_{opt}}$		ϵ	
									Experimental	Calculated	Experimental	Calculated: a. c. data	Calculated: c/4 points	Experimental	Calculated	Experimental	Calculated	Experimental	Calculated	Experimental	Calculated	Experimental	Calculated	Experimental	Calculated
00-0-0	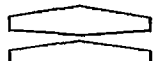	2:1	0.50	6	0015	0009	0	0	0	0	−0.014	−0.011	0	0	0	0.075	0.074	1.53	1.54	0.0076	0.0072	0.04	0	0.89	0.88
24-0-0		2:1	.50	6	2415	2409	0	0	−.040	−.043	−.022	−.012	0	−1.7	−1.7	.074	.074	1.68	1.61	.0077	.0075	.14	.13	.90	.90
24-15-0		2:1	.50	6	2415	2409	15	0	−.043	−.043	.352	.330	.345	−1.9	−1.7	.075	.074	1.63	1.61	.0076	.0075	.19	.15	.90	.90
24-30-0		2:1	.50	6	2415	2409	30	0	−.042	−.043	.775	.726	.744	−1.9	−1.7	.072	.074	1.43	1.61	.0076	.0075	.16	.12	.88	.90
24-30-8.50		2:1	.50	6	2415	2409	30	−8.50	.002	.010	.786	.725	.744	.7	.9	.076	.074	1.51	1.56	.0084	.0095	.36	.20	.92	.91
$2R_1$-15-8.50		2:1	.50	6	$2R_1$15	$2R_1$09	15	−8.50	.003	.006	.348	.330	.345	1.2	1.1	.076	.074	1.59	1.46	.0092	.0094	.26	.19	.93	.90
$2R_2$-15-0		2:1	.50	6	$2R_2$15	$2R_2$09	15	0	.004	.004	.351	.330	.345	−.7	−.6	.078	.074	1.50	1.48	.0078	.0076	.16	.10	.89	.87
00-15-3.45		2:1	.50	6	0015	0009	15	−3.45	.007	.010	.346	.331	.345	1.0	1.1	.076	.074	1.48	1.55	.0081	.0076	.06	0	.90	.88
00-15-3.45 (4:1)		4:1	.25	6	0015	0009	15	−3.45	.005	------	.334	.330	.327	.7	.5	.076	.075	1.32	1.38	.0082	.0078	.10	0	.90	.86
2218-09	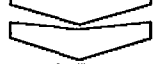	2:1	.50	6	2218	2209	0	0	−.029	−.029	−.028	−.015	0	−1.8	−1.8	.071	.075	1.60	1.61	.0088	.0085	.15	.18	.91	.90
M6		2:1	.50	6	M6 (M-18)	M6 (M-9)	0	0	−.006	.002	−.017	−.015	0	−1.1	−.7	.070	.074	1.49	1.45	.0084	.0090	.18	.05	.90	.86
Clark Y	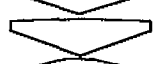	2:1	.50	6	Clark Y M-18	Clark Y M-9	0	0	−.071	−.071	−.020	−.016	0	−5.2	−5.1	.071	.074	1.67	1.61	.0091	.0095	.22	.11	.91	.89
23015-09		2:1	.50	6	23015	23009	0	0	−.007	−.007	−.014	−.012	0	−1.3	−1.1	.074	.076	1.71	1.70	.0079	.0076	.17	.11	.91	.91
23018-09		2:1	.50	6	23018	23009	0	0	−.007	−.005	−.020	−.015	0	−1.3	−1.1	.073	.075	1.66	1.63	.0085	.0084	.11	.11	.90	.89
3-10-18		3:1	.33	10	23018	23009	0	0	−.011	−.006	−.013	−.017	0	−1.2	−1.1	.083	.083	1.51	1.59	.0083	.0085	.04	.08	.80	.82
5-10-16		5:1	.20	10	23016	23009	0	0	−.009	−.007	−.011	−.016	0	−1.2	−1.1	.083	.083	1.50	1.49	.0080	.0081	.03	.10	.78	.82
5-10-18		5:1	.20	10	23018	23009	0	0	−.011	−.006	−.013	−.018	0	−1.2	−1.1	.083	.083	1.49	1.50	.0086	.0087	.05	.08	.81	.81
5-12-16	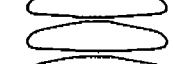	5:1	.20	12	23016	23009	0	0	−.014	−.007	−.016	−.016	0	−1.2	−1.1	.086	.085	1.46	1.49	.0079	.0081	.02	.10	.76	.79
5-12-20		5:1	.20	12	23020	23009	0	0	−.007	−.005	−.010	−.022	0	−1.2	−1.1	.084	.084	1.42	1.43	.0084	.0093	0	.08	.74	.76
0018-09		2:1	.50	6	0018	0009	0	0	0	0	−.020	−.016	0	------	------	.074	.074	1.48	1.52	.0082	.0080	0	0	.90	.87
23013-43010		1.6:1	.625	6	23013	43010	0	−2	−.009	−.011	------	−.011	0	−.7	−.5	.074	.076	1.67	1.67	.0074	.0074	------	------	------	------
Elliptical 4412	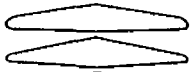	------	------	6	4412	4412	0	0	−.100	−.095	−.013	−.010	0	−4.0	−4.0	.074	.075	1.81	------	.0083	.0082	.15	.33	.92	.93

[1] All N. A. C. A. sections except the Clark Y.

slope lift curve

TABLE II

ORDINATES OF N. A. C. A. 23015-09 TAPERED AIRFOIL IN PERCENT OF CHORD

Spanwise position	0		3.000 S/b		2.660 S/b		2.787 S/b		2.914 S/b	
Stations in percent of chord	Root section		Construction tip section		Section I		Section II		Section III	
	Upper	Lower	Upper	Lower	Upper	Lower	Upper	Lower	Upper	Lower
0		0		0		0		0		0
1.25	3.34	−1.54	2.04	−.91	2.34	−1.08	2.24	−1.03	2.12	−.95
2.5	4.44	−2.26	2.83	−1.19	3.22	−1.46	3.10	−1.37	2.94	−1.29
5	5.89	−3.04	3.93	−1.44	4.44	−1.86	4.26	−1.72	4.07	−1.55
7.5	6.91	−3.61	4.70	−1.63	5.26	−2.13	5.06	−1.95	4.86	−1.76
10	7.64	−4.09	5.26	−1.79	5.84	−2.37	5.64	−2.18	5.41	−1.94
15	8.52	−4.84	5.85	−2.17	6.52	−2.84	6.29	−2.61	6.04	−2.36
20	8.92	−5.41	6.06	−2.55	6.78	−3.27	6.54	−3.02	6.26	−2.75
25	9.08	−5.78	6.11	−2.80	6.86	−3.55	6.60	−3.30	6.32	−3.02
30	9.05	−5.96	6.05	−2.96	6.80	−3.71	6.54	−3.45	6.26	−3.16
40	8.59	−5.92	5.69	−3.03	6.41	−3.75	6.16	−3.50	5.89	−3.23
50	7.74	−5.50	5.09	−2.86	5.75	−3.53	5.53	−3.30	5.26	−3.04
60	6.61	−4.81	4.32	−2.53	4.89	−3.10	4.69	−2.91	4.47	−2.69
70	5.25	−3.91	3.42	−2.08	3.88	−2.54	3.73	−2.38	3.54	−2.20
80	3.73	−2.83	2.41	−1.51	2.74	−1.85	2.63	−1.74	2.51	−1.62
90	2.04	−1.59	1.31	−.86	1.49	−1.05	1.43	−.98	1.36	−.92
95	1.12	−.90	.72	−.50	.82	−.60	.78	−.56	.74	−.52
100	.16	−.16	.10	−.10	.11	−.11	.10	−.10	.10	−.10
L. E. radius	2.48		0.89		1.21		1.10		0.98	
Slope of radius through end of chord										0.305

ORDINATES OF N. A. C. A. 23018-09 TAPERED AIRFOIL IN PERCENT OF CHORD

Spanwise position	0		3.000 S/b		2.660 S/b		2.787 S/b		2.914 S/b	
Stations in percent of chord	Root section		Construction tip section		Section I		Section II		Section III	
	Upper	Lower	Upper	Lower	Upper	Lower	Upper	Lower	Upper	Lower
0		0		0		0		0		0
1.25	4.09	−1.83	2.04	−.91	2.51	−1.17	2.34	−1.09	2.17	−.99
2.5	5.29	−2.71	2.83	−1.19	3.42	−1.59	3.23	−1.45	2.99	−1.29
5	6.92	−3.80	3.93	−1.44	4.68	−2.07	4.44	−1.84	4.15	−1.62
7.5	8.01	−4.60	4.70	−1.63	5.53	−2.33	5.26	−2.12	4.94	−1.82
10	8.83	−5.22	5.26	−1.79	6.14	−2.66	5.83	−2.36	5.49	−2.03
15	9.86	−6.18	5.85	−2.17	6.86	−3.18	6.51	−2.83	6.13	−2.45
20	10.36	−6.86	6.06	−2.55	7.15	−3.63	6.78	−3.26	6.36	−2.84
25	10.56	−7.27	6.11	−2.80	7.23	−3.93	6.85	−3.54	6.43	−3.11
30	10.55	−7.47	6.05	−2.96	7.18	−4.08	6.79	−3.70	6.36	−3.27
40	10.04	−7.37	5.69	−3.03	6.78	−4.12	6.40	−3.74	5.99	−3.33
50	9.05	−6.81	5.09	−2.86	6.08	−3.85	5.74	−3.52	5.36	−3.13
60	7.75	−5.94	4.32	−2.53	5.18	−3.39	4.88	−3.10	4.56	−2.77
70	6.18	−4.82	3.42	−2.08	4.11	−2.76	3.87	−2.52	3.61	−2.27
80	4.40	−3.48	2.41	−1.51	2.91	−2.01	2.74	−1.84	2.55	−1.66
90	2.39	−1.94	1.31	−.86	1.58	−1.13	1.50	−1.04	1.38	−.91
95	1.32	−1.09	.72	−.50	.87	−.65	.82	−.59	.76	−.54
100	.19	−.19	.10	−.10	.12	−.12	.11	−.11	.10	−.10
L. E. radius	3.56		0.89		1.39		1.21		1.02	
Slope of radius through end of chord										0.305

TABLE II—Continued

ORDINATES OF N. A. C. A. 3-10-18 TAPERED AIRFOIL IN PERCENT OF CHORD

Spanwise position	0		5.000 S/b		4.802 S/b		4.920 S/b	
Stations in percent of chord	Root section		Construction tip section		Section I		Section II	
	Upper	Lower	Upper	Lower	Upper	Lower	Upper	Lower
0		0		0		0		0
1.25	4.09	−1.83	2.04	−.91	2.24	−1.03	2.12	−.95
2.5	5.29	−2.71	2.83	−1.19	3.10	−1.37	2.94	−1.29
5	6.92	−3.80	3.93	−1.44	4.26	−1.72	4.07	−1.55
7.5	8.01	−4.60	4.70	−1.63	5.06	−1.95	4.86	−1.76
10	8.83	−5.22	5.26	−1.79	5.64	−2.18	5.41	−1.94
15	9.86	−6.18	5.85	−2.17	6.29	−2.61	6.04	−2.36
20	10.36	−6.86	6.06	−2.55	6.54	−3.02	6.26	−2.75
25	10.56	−7.27	6.11	−2.80	6.60	−3.30	6.32	−3.02
30	10.55	−7.47	6.05	−2.96	6.54	−3.45	6.26	−3.16
40	10.04	−7.37	5.69	−3.03	6.16	−3.50	5.89	−3.23
50	9.05	−6.81	5.09	−2.86	5.53	−3.30	5.26	−3.04
60	7.75	−5.94	4.32	−2.53	4.69	−2.91	4.47	−2.69
70	6.18	−4.82	3.42	−2.08	3.73	−2.38	3.54	−2.20
80	4.40	−3.48	2.41	−1.51	2.63	−1.74	2.51	−1.62
90	2.39	−1.94	1.31	−.86	1.43	−.98	1.36	−.92
95	1.32	−1.09	.72	−.50	.78	−.56	.74	−.52
100	.19	−.19	.10	−.10	.10	−.10	.10	−.10
L. E. radius	3.56		0.89		1.10		0.98	
Slope of radius through end of chord								0.305

ORDINATES OF N. A. C. A. 5-10-16 TAPERED AIRFOIL IN PERCENT OF CHORD

Spanwise position	0		5.000 S/b		4.840 S/b		4.938 S/b	
Stations in percent of chord	Root section		Construction tip section		Section I		Section II	
	Upper	Lower	Upper	Lower	Upper	Lower	Upper	Lower
0		0		0		0		0
1.25	3.59	−1.64	2.04	−.91	2.24	−1.03	2.12	−.95
2.5	4.71	−2.39	2.83	−1.19	3.10	−1.37	2.94	−1.29
5	6.22	−3.31	3.93	−1.44	4.26	−1.72	4.07	−1.55
7.5	7.28	−3.94	4.70	−1.63	5.06	−1.95	4.86	−1.76
10	8.03	−4.47	5.26	−1.79	5.64	−2.18	5.41	−1.94
15	8.97	−5.29	5.85	−2.17	6.29	−2.61	6.04	−2.36
20	9.40	−5.90	6.06	−2.55	6.54	−3.02	6.26	−2.75
25	9.57	−6.27	6.11	−2.80	6.60	−3.30	6.32	−3.02
30	9.55	−6.46	6.05	−2.96	6.54	−3.45	6.26	−3.16
40	9.07	−6.40	5.69	−3.03	6.16	−3.50	5.89	−3.23
50	8.18	−5.94	5.09	−2.86	5.53	−3.30	5.26	−3.04
60	6.99	−5.18	4.32	−2.53	4.69	−2.91	4.47	−2.69
70	5.57	−4.21	3.42	−2.08	3.73	−2.38	3.54	−2.20
80	3.96	−3.04	2.41	−1.51	2.63	−1.74	2.51	−1.62
90	2.15	−1.70	1.31	−.86	1.43	−.98	1.36	−.92
95	1.19	−.97	.72	−.50	.78	−.56	.74	−.52
100	.17	−.17	.10	−.10	.10	−.10	.10	−.10
L. E. radius	2.82		0.89		1.10		0.98	
Slope of radius through end of chord								0.305

TABLE II—Continued

ORDINATES OF N. A. C. A. 5-10-18 TAPERED AIRFOIL IN PERCENT OF CHORD

Spanwise position	0		5.000 S/b		4.880 S/b		4.952 S/b	
Stations in percent of chord	Root section		Construction tip section		Section I		Section II	
	Upper	Lower	Upper	Lower	Upper	Lower	Upper	Lower
0		0		0		0		0
1.25	4.09	−1.83	2.04	−.91	2.24	−1.03	2.12	−.95
2.5	5.29	−2.71	2.83	−1.19	3.10	−1.37	2.94	−1.29
5	6.92	−3.80	3.93	−1.44	4.26	−1.72	4.07	−1.55
7.5	8.01	−4.60	4.70	−1.63	5.06	−1.95	4.86	−1.76
10	8.83	−5.22	5.26	−1.79	5.64	−2.18	5.41	−1.94
15	9.86	−6.18	5.85	−2.17	6.29	−2.61	6.04	−2.36
20	10.36	−6.86	6.06	−2.55	6.54	−3.02	6.26	−2.75
25	10.56	−7.27	6.11	−2.80	6.60	−3.30	6.32	−3.02
30	10.55	−7.47	6.05	−2.96	6.54	−3.45	6.26	−3.16
40	10.04	−7.37	5.69	−3.03	6.16	−3.50	5.89	−3.23
50	9.05	−6.81	5.09	−2.86	5.53	−3.30	5.26	−3.04
60	7.75	−5.94	4.32	−2.53	4.69	−2.91	4.47	−2.69
70	6.18	−4.82	3.42	−2.08	3.73	−2.38	3.54	−2.20
80	4.40	−3.48	2.41	−1.51	2.63	−1.74	2.51	−1.62
90	2.39	−1.94	1.31	−.86	1.43	−.98	1.36	−.92
95	1.32	−1.09	.72	−.50	.78	−.56	.74	−.52
100	.19	−.19	.10	−.10	.10	−.10	.10	−.10
L. E. radius	3.56		0.89		1.10		0.98	
Slope of radius through end of chord							0.305	

ORDINATES OF N. A. C. A. 5-12-16 TAPERED AIRFOIL IN PERCENT OF CHORD

Spanwise position	0		6.000 S/b		5.844 S/b		5.925 S/b	
Stations in percent of chord	Root section		Construction tip section		Section I		Section II	
	Upper	Lower	Upper	Lower	Upper	Lower	Upper	Lower
0		0		0		0		0
1.25	3.59	−1.64	2.04	−.91	2.20	−1.00	2.12	−.95
2.5	4.71	−2.39	2.83	−1.19	3.05	−1.34	2.94	−1.29
5	6.22	−3.31	3.93	−1.44	4.23	−1.67	4.07	−1.55
7.5	7.28	−3.94	4.70	−1.63	5.01	−1.89	4.86	−1.76
10	8.03	−4.47	5.26	−1.79	5.59	−2.11	5.41	−1.94
15	8.97	−5.29	5.85	−2.17	6.21	−2.53	6.04	−2.36
20	9.40	−5.90	6.06	−2.55	6.45	−2.94	6.26	−2.75
25	9.57	−6.27	6.11	−2.80	6.52	−3.21	6.32	−3.02
30	9.55	−6.46	6.05	−2.96	6.46	−3.36	6.26	−3.16
40	9.07	−6.40	5.69	−3.03	6.08	−3.42	5.89	−3.23
50	8.18	−5.94	5.09	−2.86	5.45	−3.22	5.26	−3.04
60	6.99	−5.18	4.32	−2.53	4.63	−2.84	4.47	−2.69
70	5.57	−4.21	3.42	−2.08	3.67	−2.33	3.54	−2.20
80	3.96	−3.04	2.41	−1.51	2.60	−1.70	2.51	−1.62
90	2.15	−1.70	1.31	−.86	1.41	−.96	1.36	−.92
95	1.19	−.97	.72	−.50	.77	−.55	.74	−.52
100	.17	−.17	.10	−.10	.10	−.10	.10	−.10
L. E. radius	2.82		0.89		1.06		0.93	
Slope of radius through end of chord							0.305	

TABLE II—Continued

ORDINATES OF N. A. C. A. 5-12-20 TAPERED AIRFOIL IN PERCENT OF CHORD

Spanwise position	0		6.000 S/b		5.833 S/b		5.953 S/b	
Stations in percent of chord	Root section		Construction tip section		Section I		Section II	
	Upper	Lower	Upper	Lower	Upper	Lower	Upper	Lower
0		0		0		0		0
1.25	4.60	−2.00	2.04	−.91	2.24	−1.03	2.12	−.95
2.5	5.84	−3.00	2.83	−1.19	3.10	−1.37	2.94	−1.29
5	7.58	−4.30	3.93	−1.44	4.26	−1.72	4.07	−1.55
7.5	8.76	−5.22	4.70	−1.63	5.06	−1.95	4.86	−1.76
10	9.64	−5.97	5.26	−1.79	5.64	−2.18	5.41	−1.94
15	10.75	−7.07	5.85	−2.17	6.29	−2.61	6.04	−2.36
20	11.30	−7.81	6.06	−2.55	6.54	−3.02	6.26	−2.75
25	11.56	−8.25	6.11	−2.80	6.60	−3.30	6.32	−3.02
30	11.55	−8.46	6.05	−2.96	6.54	−3.45	6.26	−3.16
40	11.00	−8.33	5.69	−3.03	6.16	−3.50	5.89	−3.23
50	9.96	−7.71	5.09	−2.86	5.53	−3.30	5.26	−3.04
60	8.51	−6.71	4.32	−2.53	4.69	−2.91	4.47	−2.69
70	6.79	−5.42	3.42	−2.08	3.73	−2.38	3.54	−2.20
80	4.83	−3.92	2.41	−1.51	2.63	−1.74	2.51	−1.62
90	2.64	−2.18	1.31	−.86	1.43	−.98	1.36	−.92
95	1.45	−1.23	.72	−.50	.78	−.56	.74	−.52
100	.21	−.21	.10	−.10	.10	−.10	.10	−.10
L. E. radius	4.40		0.89		1.10		0.98	
Slope of radius through end of chord								0.305

TABLE III

ORDINATES OF N. A. C. A. CENTER-STALLING WING

DATA ON SECTIONS

[Total geometric washout, 3.2°; total aerodynamic washout, 2° at construction tip]

Section	Root	1	2	3	4	5	6	7	8
Position, fraction semispan	0	0.200	0.400	0.600	0.802	0.853	0.900	0.940	0.973
Geometric washout, degrees	0	.37	.89	1.47	2.24	2.47	2.70	2.91	3.02

ORDINATES

[Percent of chord]

Root section				Section 1			
Upper surface		Lower surface		Upper surface		Lower surface	
Station	Ordinate	Station	Ordinate	Station	Ordinate	Station	Ordinate
0	0	0	0	0	0	0	0
.72	2.34	1.78	−1.63	.68	2.31	1.82	−1.50
1.87	3.43	3.13	−2.10	1.81	3.41	3.19	−1.90
4.38	4.96	5.62	−2.64	4.32	4.98	5.68	−2.35
7.01	6.02	7.99	−3.03	6.96	6.07	8.04	−2.68
9.69	6.76	10.31	−3.36	9.66	6.83	10.34	−2.97
15.00	7.63	15.00	−3.95	15.00	7.70	15.00	−3.52
20.14	7.98	19.86	−4.45	20.15	8.02	19.85	−4.01
25.14	8.09	24.86	−4.78	25.16	8.11	24.84	−4.35
30.14	8.05	29.86	−4.95	30.16	8.05	29.84	−4.54
40.14	7.61	39.86	−4.96	40.15	7.59	39.85	−4.58
50.13	6.84	49.87	−4.63	50.14	6.81	49.86	−4.30
60.11	5.83	59.89	−4.06	60.12	5.79	59.88	−3.78
70.09	4.63	69.91	−3.30	70.10	4.60	69.90	−3.09
80.06	3.28	79.94	−2.40	80.07	3.25	79.93	−2.25
90.04	1.79	89.96	−1.35	90.04	1.77	89.96	−1.27
95.02	.98	94.98	−.76	95.02	.97	94.98	−.72
100.00	.14	100.00	−.14	100.00	.13	100.00	−.13
L. E. radius 1.859 on 0.305 slope				L. E. radius 1.744 on 0.346 slope			

Section 2				Section 3			
Upper surface		Lower surface		Upper surface		Lower surface	
Station	Ordinate	Station	Ordinate	Station	Ordinate	Station	Ordinate
0	0	0	0	0	0	0	0
.63	2.27	1.87	−1.35	.58	2.22	1.92	−1.17
1.75	3.39	3.25	−1.67	1.69	3.37	3.31	−1.40
4.26	5.01	5.74	−2.01	4.19	5.04	5.81	−1.61
6.92	6.13	8.08	−2.27	6.86	6.21	8.14	−1.78
9.62	6.91	10.38	−2.51	9.59	7.02	10.41	−1.97
15.00	7.77	15.00	−3.01	15.00	7.88	15.00	−2.42
20.16	8.07	19.84	−3.50	20.18	8.15	19.82	−2.90
25.17	8.14	24.83	−3.85	25.19	8.18	24.81	−3.26
30.17	8.06	29.83	−4.06	30.19	8.07	29.81	−3.48
40.17	7.57	39.83	−4.14	40.18	7.55	39.82	−3.62
50.15	6.77	49.85	−3.91	50.17	6.74	49.83	−3.46
60.13	5.75	59.87	−3.46	60.14	5.71	59.86	−3.08
70.11	4.55	69.89	−2.84	70.12	4.51	69.88	−2.54
80.08	3.22	79.92	−2.07	80.08	3.18	79.92	−1.87
90.04	1.75	89.96	−1.17	90.05	1.72	89.95	−1.07
95.02	.96	94.98	−.67	95.02	.94	94.98	−.61
100.00	.13	100.00	−.13	100.00	.12	100.00	−.12
L. E. radius 1.613 on 0.395 slope				L. E. radius 1.470 on 0.453 slope			

ORDINATES—Continued

Section 4				Section 5			
Upper surface		Lower surface		Upper surface		Lower surface	
Station	Ordinate	Station	Ordinate	Station	Ordinate	Station	Ordinate
0	0	0	0	0	0	0	0
.54	2.17	1.96	−.95	.53	2.15	1.97	−.88
1.63	3.34	3.37	−1.06	1.62	3.33	3.38	−.96
4.13	5.08	5.87	−1.11	4.12	5.09	5.88	−.97
6.81	6.30	8.19	−1.17	6.80	6.32	8.20	−1.00
9.55	7.13	10.45	−1.29	9.54	7.16	10.46	−1.10
15.00	7.99	15.00	−1.67	15.00	8.02	15.00	−1.46
20.20	8.22	19.80	−2.15	20.20	8.24	19.80	−1.94
25.20	8.21	24.80	−2.52	25.21	8.22	24.79	−2.31
30.21	8.08	29.79	−2.77	30.21	8.08	29.79	−2.57
40.20	7.52	39.80	−2.97	40.20	7.51	39.80	−2.78
50.18	6.68	49.82	−2.89	50.18	6.66	49.82	−2.72
60.16	5.64	59.84	−2.60	60.16	5.62	59.84	−2.47
70.13	4.45	69.87	−2.17	70.13	4.43	69.87	−2.07
80.09	3.13	79.91	−1.61	80.09	3.11	79.91	−1.54
90.05	1.69	89.95	−.93	90.05	1.68	89.95	−.89
95.03	.92	94.97	−.54	95.03	.91	94.97	−.52
100.00	.11	100.00	−.11	100.00	.11	100.00	−.11
L. E. radius 1.295 on 0.524 slope				L. E. radius 1.248 on 0.544 slope			

Section 6				Section 7			
Upper surface		Lower surface		Upper surface		Lower surface	
Station	Ordinate	Station	Ordinate	Station	Ordinate	Station	Ordinate
0	0	0	0	0	0	0	0
.52	2.14	1.98	−.82	.52	2.12	1.98	−.77
1.61	3.32	3.39	−.87	1.60	3.32	3.40	−.78
4.10	5.10	5.90	−.83	4.09	5.11	5.91	−.70
6.79	6.34	8.21	−.83	6.78	6.37	8.22	−.68
9.54	7.20	10.46	−.91	9.53	7.23	10.47	−.74
15.00	8.06	15.00	−1.26	15.00	8.09	15.00	−1.07
20.20	8.26	19.80	−1.73	20.21	8.28	19.79	−1.54
25.21	8.23	24.79	−2.11	25.21	8.24	24.79	−1.92
30.21	8.08	29.79	−2.37	30.22	8.08	29.78	−2.19
40.21	7.50	39.79	−2.60	40.21	7.50	39.79	−2.44
50.19	6.65	49.81	−2.56	50.19	6.64	49.81	−2.42
60.16	5.60	59.84	−2.34	60.16	5.59	59.84	−2.22
70.13	4.41	69.87	−1.96	70.13	4.40	69.87	−1.87
80.09	3.10	79.91	−1.46	80.10	3.09	79.90	−1.10
90.05	1.67	89.95	−.85	90.05	1.66	89.95	−.82
95.03	.90	94.97	−.50	95.03	.90	94.97	−.48
100.00	.11	100.00	−.11	100.00	.11	100.00	−.11
L. E. radius 1.201 on 0.564 slope				L. E. radius 1.162 on 0.582 slope			

Section 8			
Upper surface		Lower surface	
Station	Ordinate	Station	Ordinate
0	0	0	0
.51	2.12	1.99	−.73
1.59	3.32	3.41	−.72
4.08	5.13	5.92	−.60
6.77	6.40	8.23	−.56
9.52	7.26	10.48	−.61
15.00	8.13	15.00	−.93
20.21	8.31	19.79	−1.40
25.22	8.27	24.78	−1.78
30.22	8.10	29.78	−2.05
40.21	7.50	39.79	−2.32
50.19	6.64	49.81	−2.32
60.17	5.59	59.83	−2.13
70.13	4.40	69.87	−1.80
80.10	3.08	79.90	−1.35
90.05	1.66	89.95	−.79
95.03	.90	94.97	−.47
100.00	.11	100.00	−.11
L. E. radius 1.135 on 0.597 slope			

TABLE IV

CALCULATION OF C_{D_0}

[N. A. C. A. 5-10-18 wing. R_s (based on $\frac{S}{b}$) = 6,630,000]

1	2	3	4	5	6	7	8	9	10	11
Fraction semispan, $\frac{y}{b/2}$	$\frac{\text{Thickness}}{\text{Chord}}, \frac{t}{c}$	Chord length, c (inches)	R_s (millions)	$(c_{l_{max}})_{std}$ (R_s=8,200,000)	$\Delta c_{l_{max}}$	$c_{l_{max}}$	$(c_{d_{0_{min}}})_{std}$ (R_s=8,200,000)	$c_{d_{0_{min}}}$	$c_{l_{opt}}$	$c_{l_{max}}-c_{l_{opt}}$
0	0.180	6.48	11.10	1.59	0	1.59	0.0091	0.0068	0.08	1.51
.2	.176	5.44	9.30	1.61	0	1.61	.0089	.0088	.08	1.53
.4	.170	4.40	7.53	1.65	0	1.65	.0087	.0088	.08	1.57
.6	.160	3.37	5.76	1.69	−.05	1.64	.0084	.0087	.09	1.55
.8	.140	2.33	3.98	1.75	−.12	1.63	.0077	.0083	.10	1.53
.9	.122	1.82	3.11	1.75	−.17	1.58	.0071	.0079	.10	1.48
.95	.109	1.56	2.66	1.74	−.22	1.52	.0068	.0077	.11	1.41

1	12	13	14	15	16	17	18	19
Fraction semispan, $\frac{y}{b/2}$	L_a	$\frac{S}{cb}L_a=c_{l_{al}}$	$0.8\times c_{l_{al}}=c_l$	$c_l-c_{l_{opt}}$	$\frac{\lvert c_l-c_{l_{opt}}\rvert}{c_{l_{max}}-c_{l_{opt}}}$	Δc_{d_0}	$c_{d_{0_{min}}}+\Delta c_{d_0}=c_{d_0}$	$c_{d_0}\times c$
0	1.473	0.881	0.705	0.625	0.414	0.0032	0.0120	0.0777
.2	1.347	.959	.767	.687	.449	.0037	.0125	.0680
.4	1.167	1.026	.821	.741	.472	.0041	.0129	.0568
.6	.929	1.069	.855	.765	.494	.0046	.0133	.0448
.8	.653	1.086	.869	.769	.503	.0047	.0130	.0303
.9	.472	1.007	.806	.706	.477	.0042	.0121	.0220
.95	.346	.862	.690	.580	.411	.0031	.0108	.0168